cells. 11β-HSD1 expression increases with age in primary dermal fibroblasts and in skin tissues [15,16]. Furthermore, Cirillo et al. demonstrated enzymatic activity of 11β-HSDs in keratinocyte in culture [17]. While these results suggested that 11β-HSDs have functions in skin component cells, the *in vivo* functions of 11β-HSDs, in skin homeostasis remained unclear.

In this study, we demonstrate that 11β-HSD1 is critical for skin homeostasis, which functions by modulating keratinocyte and fibroblast proliferation. In addition, we show the effect of topical application of a selective inhibitor of 11β-HSD1 on mouse skin and cutaneous wound healing, which collectively may demonstrate the possibility of 11β-HSD1 as a novel target in treating cutaneous disease.

Materials and Methods

Cell culture

Normal human epidermal keratinocytes (NHEKs) and normal human dermal fibroblasts (NHDFs) were purchased from DS Pharma Biomedical (Osaka, Japan). NHEKs were cultured on type-1 collagen-coated plates (Asahi Techno Glass, Funabashi, Japan) in human keratinocyte serum-free medium (DS Pharma Biomedical) supplemented with bovine pituitary extract. Dulbecco's modified Eagle's medium (DMEM) containing 10% fetal bovine serum (FBS) was used to culture NHDFs. Isolation and culture of mouse keratinocytes and mouse fibroblasts were carried out as previously described [18]. Full-thickness skin harvested from day 2 to day 4 newborn mice was treated with 4 mg/ml of dispase (Gibco; Invitrogen, Paisley, UK) for 1 h at 37°C. Next, the epidermis was peeled from the dermis. The epidermis was trypsinized to prepare single cells. It was then incubated in Human Keratinocyte Serum Free Medium for 6 h at 37°C under an atmosphere with 5% CO_2. Non-adherent cells were washed away with phosphate-buffered saline (PBS) twice, and then cultured for 2–3 days in human keratinocyte serum free medium before use in experiments. The dermis was placed in PBS+0.05% type-1 collagenase (Sigma-Aldrich, St Louis, MO, USA) and incubated at 37°C for 30 min with vigorous agitation to prepare single cells. After filtration, cells were centrifuged at 200 g for 10 min, resuspended in DMEM+10% FBS, and incubated at 37°C and in 5% CO_2. First or second passage fibroblasts were used for experiments.

Histopathological analysis

Samples of normal skin from healthy volunteers were taken after written informed consent. All studies were approved by the ethical committee of Osaka University. Samples were fixed in 10% formaldehyde for 24 h, followed by embedding in paraffin and microtome sectioning. Slides were stained with hematoxylin and eosin (H&E). For immunohistochemical analysis, sections were hydrated by passage through xylene and graded ethanols. After antigen retrieval for 10 min at 90°C in citric buffer, pH 6.0, the slides were blocked with serum-free protein block (Dako-Cytomation, Carpinteria, CA, USA) for 10 min, then incubated with primary antibody overnight at 4°C (rabbit anti-11β-HSD1 antibody 1:100 dilution, Abcam, Cambridge, UK; rabbit anti-Ki-67 antibody 1:500 dilution, Novocastra Laboratories Ltd, Newcastle, UK). After washing with tris-buffered saline (TBS) containing 0.05% Triton-X100, slides were mounted using the Vectastain ABC kit® (Vector Laboratories, Burlingame, CA, USA) followed by counterstaining with haematoxylin. Rabbit IgG were used as the isotype controls. For immunofluorescent analysis, sections were hydrated as described above and incubated with primary antibody (rabbit anti-11β-HSD1 antibody 1:100 dilution and mouse anti-keratin 14 antibody 1:500 dilution, Abcam), followed by secondary antibody (anti-rabbit Alexa Fluor 555 and anti-mouse Alexa Fluor 488, Invitrogen).

Western blotting

Cell samples were solubilized at 4°C in lysis buffer (0.5% sodium deoxycholate, 1% Nonidet P40, 0.1% sodium dodecyl sulphate, 100 μg/ml phenylmethylsulphonyl fluoride, 1 mM sodium orthovanadate, and protease inhibitor cocktail). For *in vivo* samples, skins were crushed in liquid nitrogen and solubilized at 4°C in lysis buffer. Ten micrograms of protein were separated on SDS-polyacrylamide gels and transferred onto polyvinylidine fluoride membranes (Bio-Rad, Hercules, CA, USA). Non-specific protein binding was blocked by incubating the membranes in 5% w/v non-fat milk powder in TBS-T (50 mM Tris-HCl, pH 7.6, 150 mM NaCl, and 0.1% v/v Tween-20). The membranes were incubated with sheep anti-11β-HSD1 antibody (The Binding Site, Birmingham, UK), rabbit anti-keratin 1 antibody (Covance, Emeryville, CA, USA), and anti-involucrin (IVL) antibody (Santa Cruz Biotechnology, Santa Cruz, CA, USA) at a dilution of 1:1000 overnight at 4°C or with mouse monoclonal anti-β-actin (Sigma-Aldrich, St. Louis, MO, USA) at a dilution of 1:5000 for 30 min at room temperature. Then, the membranes were washed three times in TBS-T for 5 min. Finally, the membranes were incubated with either HRP-conjugated anti-rabbit, anti-mouse, or anti-sheep antibody at a dilution of 1:10,000 for 60 min at room temperature. Protein bands were detected using the ECL Plus kit (GE Healthcare, Buckinghamshire, UK). The intensity of the bands was quantified by using NIH image J software.

11β-HSD1 inhibitor treatment

11β-HSD1 inhibitor (385581) purchased from Merck (Whitehouse Station, NJ, USA) is a potent inhibitor of 11β-HSD1 with >450- and >100-fold selectivity over human and mouse 11β-HSD2, respectively [19]. The inhibitor was dissolved in DMSO and further diluted more than 100,000-fold in culture medium (for *in vitro* experiments), in a 1:1 mixture of acetone:olive oil (for *in vivo* topical application), or in PBS (for *in vivo* wound healing). DMSO was used as a vehicle control.

MTS cell viability assay

Cellular viability was assessed using CellTiter96® Aqueous One Solution Cell Proliferation Assay (Promega, Madison, WI, USA). Briefly, NHEKs or NHDFs were seeded onto 96-well plates (5000 cells/well or 500 cells/well in 100 μl medium, respectively). The cells were allowed to attach for 24 h and then incubated with 11β-HSD1 inhibitor or vehicle control at the indicated doses for 48 h. Next, 20 μl of MTS reagent was added, and the cells were incubated for 2 h. Optical density was measured at 490 nm with a Micro Plate Reader (Bio-Rad, Hercules, CA, USA).

BrdU incorporation assay

Cell proliferation was assessed using cell proliferation ELISA, BrdU (Roche, Basel, Switzerland) according to the manufacturer's protocol. Briefly, NHEKs were seeded onto 96-well plates (5000 cells/well in 100 μl medium). The cells were allowed to attach for 24 h and then incubated with 11β-HSD1 inhibitor or vehicle control at the indicated doses for 48 h. Next, cells were labeled with BrdU, and incubated for 4 h. BrdU incorporation was quantified by measuring with a Micro Plate Reader (Bio-Rad) at 450 nm.

siRNA transfection

NHEKs (50,000 cells/ml) were seeded on type-1 collagen coated plates 1 day prior to transfection. Cells were transfected with 11β-HSD1 or control siRNAs (Invitrogen) at 50 nM using RNAi MAX (Invitrogen), and the culture medium was replaced 6 h later. Cells were used for experiments 48 h after transfection.

RNA isolation and quantitative real time polymerase chain reaction (rtPCR)

Total RNA was isolated from cells using the SV Total RNA Isolation System (Promega). The product was reverse-transcribed into first-strand complementary DNA (cDNA). Thereafter, the expression of 11β-HSD1, 11β-HSD2, IVL, and keratin 10 (K10) was measured using the Power SYBR Green PCR Master Mix (Applied Biosystems, Foster City, CA) according to the manufacturer's protocol. Glyceraldehyde-3-phosphate dehydrogenase (GAPDH) was used to normalize the mRNA as quantified GAPDH was not affected by the treatment. Similar results were obtained in each experiment when another internal control, β-actin, was used to normalize the mRNA (data not shown). Sequence-specific primers were designed as follows: 11β-HSD1, sense: 5′-tctcctctctggctgggaaag, antisense: 5′- gaacccatccaaagcaaacttg; IVL, sense: 5′-tctgcctcagccttactgtg, antisense: 5′-ggaggaggaacagtcttgagg; K10, sense: 5′-tgaaaagcatggcaactcac, antisense: 5′-tgtcgatctgaagcaggatg; Fibroblast growth factor-2 (FGF-2), sense: 5′-agagcgaccctcacatcaag, antisense: 5′- actgcccagttcgtttcagt; TGF-β, sense: 5′- cacgtggagctgtaccagaa: 5′- gaacccgttgatgtccactt ; Matrix metalloproteinase-1 (MMP-1), sense: 5′- gtgctaaaggtgccaatggt, antisense: 5′- tccttggggtatccgtgtag ; Collagen 1 alpha 1 (Col1a1), sense: 5′- ctcctcgctttccttcctct, antisense: 5′- ctcctcgctttccttcctct ; and GAPDH, sense: 5′- ggagtcaacggatttggtcgta-3′, antisense: 5′- gcaacaatatccactttaccagagttaa-3′. Real-time PCR (40 cycles of denaturation at 92°C for 15 seconds and annealing at 60°C for 60 seconds) was run on an ABI 7000 Prism (Applied Biosystems). Samples without reverse transcriptase (negative control) did not show any amplification.

Cortisol measurement by ELISA

NHEKs (10,000 cells/ml, 100 μl) were seeded on 96-well type-A collagen-coated plates. The cells were allowed to attach for 24 h and then the medium was changed to a high calcium (1.2 mM) basal medium that did not contain bovine pituitary extract, to remove cortisol from the culture media. The culture media were harvested 48 h later. Harvested samples were stored at −20°C until use. The amount of cortisol in samples was measured with an Cortisol EIA kit (Cayman Chemical Company, Ann Arbor, MI, USA).

Wound healing assay

Male C57BL/6 and C57BL/6J-*ob/ob* mice were obtained from Japan Charles River, Inc. Animal care was in accordance with the institutional guidelines of Osaka University. At 6 weeks of age, dorsal hairs were removed by using hair removal cream (epilat, Kracie, Inc., Tokyo, Japan). Full-thickness 15-mm wounds were created on the backs of mice (n = 3 in each group for first experiment and n = 4 in each group for second experiment) a day after hair removal. 11β-HSD1 inhibitor (10 μM) or vehicle control dissolved in PBS was applied to the wound and the wound was covered with hydrocolloid dressing. This application was repeated every 2 days. The wound areas were calculated by measuring the major and minor axes on days, 0, 2, 4, 6, 8, 10, and 12 after wounds were created.

Topical 11β-HSD1 inhibitor treatment

Eight-week-old male Hos: HR-1 mice (hairless mice) were obtained from Japan SLC, Inc. Animal care was in accordance with the institutional guidelines of Osaka University. Mouse dorsal skins (n = 3 in each group for first experiment and n = 5 in each group for second experiment) were treated with 11β-HSD1 inhibitor (50 μM) or vehicle control dissolved in a 1:1 mixture of acetone:olive oil for 5 continuous days. One day after the last treatment, the treated dorsal skins were harvested for histological analysis.

Statistical analysis

The data are expressed as mean values ± standard deviation (SD). The unpaired Student's *t*-test was used to determine the level of significance of differences between the sample means.

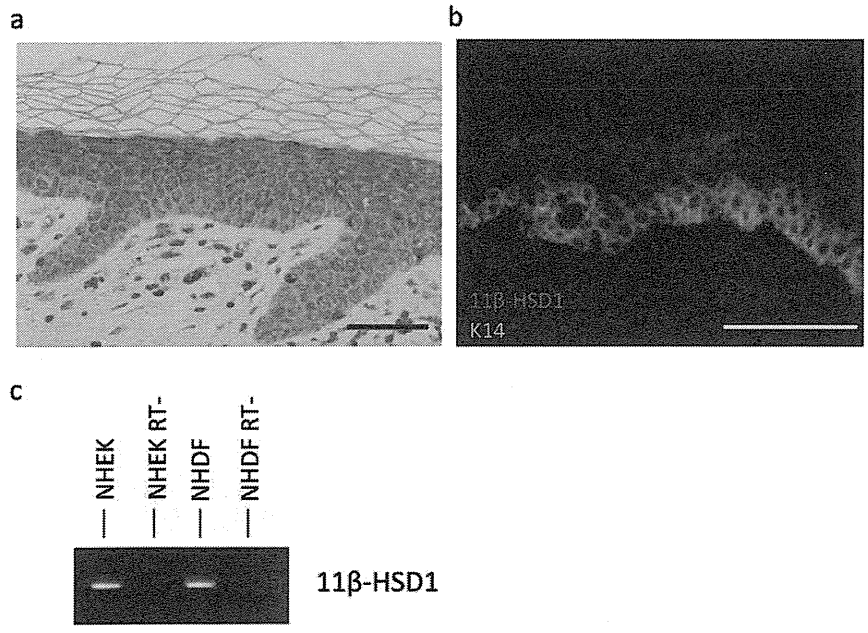

Figure 1. 11β-HSD1 expression in human skin. (a) Immunohistochemical staining of 11β-HSD1 (DAB staining) in normal skin tissue. Bar = 50 μM (b) Immunofluorescent staining of 11β-HSD1 (red) and keratin 14 (green). Bar = 100 μM (c) PCR detecting 11β-HSD1 in NHEKs and NHDFs. RT-: samples without reverse transcriptase (negative control).
doi:10.1371/journal.pone.0025039.g001

Results

11β-HSD1 expression in the skin

First, the expression of 11β-HSD1 in healthy skin was examined. 11β-HSD1 was broadly expressed in all layers of the epidermis and in dermal fibroblasts (Figure 1a). Its expression was stronger in the cytoplasm of supra-basal cells, and only weakly detected in basal cells. This was also confirmed by double staining with both the anti-11β-HSD1 antibody and the basal cell marker, anti-K14 (Figure 1b). The expression of 11β-HSD1 was also detected in cultured NHEKs and in NHDFs (Figure 1c).

11β-HSD1 expression is increased by starvation or calcium induced differentiation

We next investigated whether the starvation and differentiation alter the expression of 11β-HSD1 in NHEKs. Starving keratinocytes by depriving them of pituitary extract in the culture media retards the growth of keratinocytes. Twenty-four hours of starvation significantly increased the expression of 11β-HSD1 (Figure 2a). NHEKs are known to differentiate when 1.2 mM calcium is added. This treatment causes the early differentiation markers keratin 1 (K1), K10, and IVL to increase as the cells differentiate [20,21]. The stimulation of differentiation with 1.2 mM of calcium increased the expression of 11β-HSD1 in NHEKs (Figure 2b and 2c). These results indicate that starvation of essential supplements or calcium-induced differentiation increases the expression of 11β-HSD1 in NHEKs.

11β-HSD1 regulates proliferation, but not differentiation, of NHEKs

To determine if 11β-HSD1 modulated keratinocyte proliferation, we investigated the effect of selective 11β-HSD1 inhibitor on the

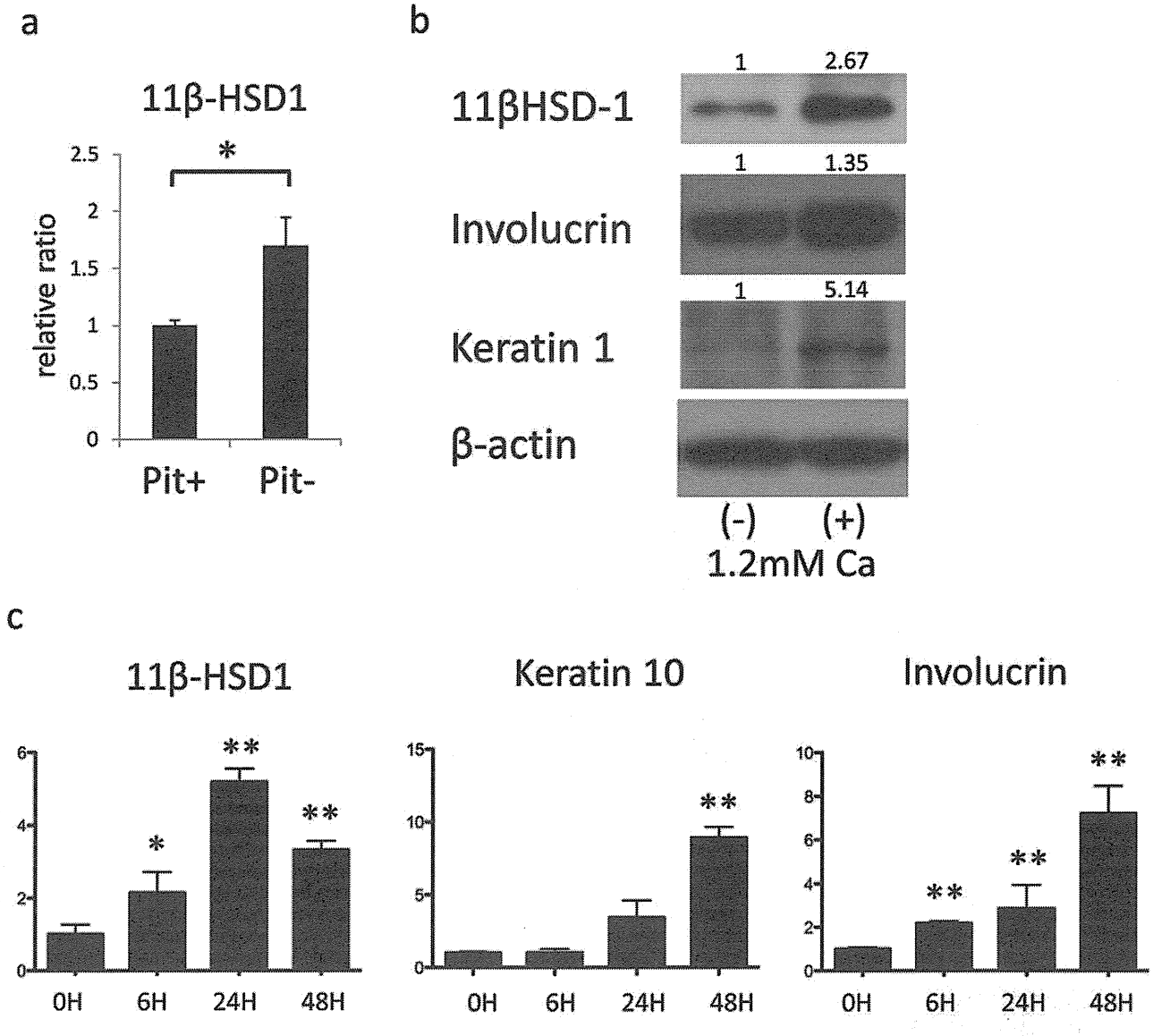

Figure 2. 11β-HSD1 expression is increased with starvation and differentiation. (a) The relative expression of 11β-HSD1 in NHEKs assessed by rtPCR with or without pituitary extract (pit) in culture media. GAPDH was used as an internal control. (b)Western blotting for detecting 11β-HSD1, Keratin 1, and Involucrin 48 h after adding 1.2 mM of calcium to culture media of NHEKs. The numbers indicate the relative ratio to β-actin. (c) The relative expressions of 11β-HSD1, Keratin 10, and Involucrin of the indicated hour after adding 1.2 mM calcium to culture media of NHEKs assessed by rtPCR. GAPDH was used as an internal control. An asterisk indicates a statistically significant difference (*P<0.05, **P<0.01, Student's *t*-test).
doi:10.1371/journal.pone.0025039.g002

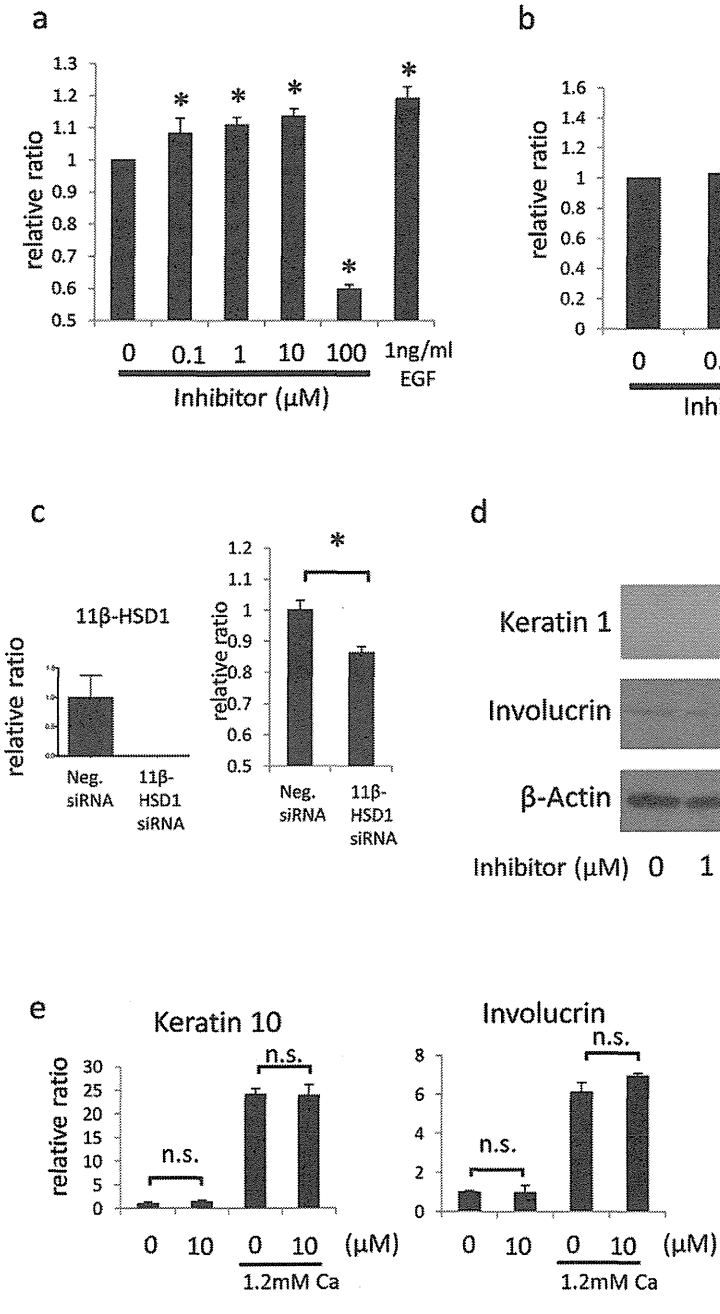

Figure 3. 11β-HSD1 regulates proliferation but not differentiation of NHEKs. (a,b) 11β-HSD1 selective inhibitor was applied to NHEKs at indicated dose and proliferation of the cells was assessed by MTS assay (a) and BrdU absorption (b) 72 h later. DMSO was applied as vehicle control and epidermal growth factor (EGF) was used as positive control in MTS assay. The relative ratio compared with absorbance of vehicle control (0 μM) is suggested. The histograms indicate means and SDs for eight independent experiments. An asterisk (*) indicates a statistically significant difference from the vehicle treated group ($P<0.05$, Student's *t*-test). (c) siRNA knockdown efficacy (left) and MTS assay (right) of NHEKs transfected with 11β-HSD1 or control. Assay was performed 48 h after transfection. Transfection of si11β-HSD1 decreased the mRNA expression 11β-HSD1 more than 95% assessed by rtPCR. GAPDH was used as an internal control. The histograms indicate means and SDs for eight independent experiments. An asterisk (*) indicates a statistically significant difference from the vehicle treated group ($P<0.05$, Student's *t*-test). (d) Western blotting of NHEKs for detecting Keratin 1, and Involucrin treated with 11β-HSD1 selective inhibitor at indicated dose for 72 h with or without 1.2 mM calcium treatment. β-actin was used as an internal control. (e) The relative expressions of Keratin 10 and Involucrin treated with 10 μM 11β-HSD1 selective inhibitor for 48 h with or without 1.2 mM calcium treatment assessed by rtPCR. GAPDH was used as an internal control. n.s.: not significant.
doi:10.1371/journal.pone.0025039.g003

proliferation of NHEKs. Addition of 100 nM–10 μM of inhibitor to culture medium, induced cell proliferation in a dose dependent manner in both MTS assays (Figure 3a) and BrdU absorption assays (Figure 3b), suggesting that 11β-HSD1 inhibits keratinoctye proliferation. In contrast, higher doses (100 μM) of inhibitor decreased cell viability. Knocking down 11β-HSD1 with siRNA also reduced the viability of NHEKs (Figure 3c). These observations suggest that basal levels of 11β-HSD1 are essential for keratinocytes survival, and excessive loss of 11β-HSD1 activity with higher doses of inhibitor (100 μM) or siRNA-mediated depletion, can therefore

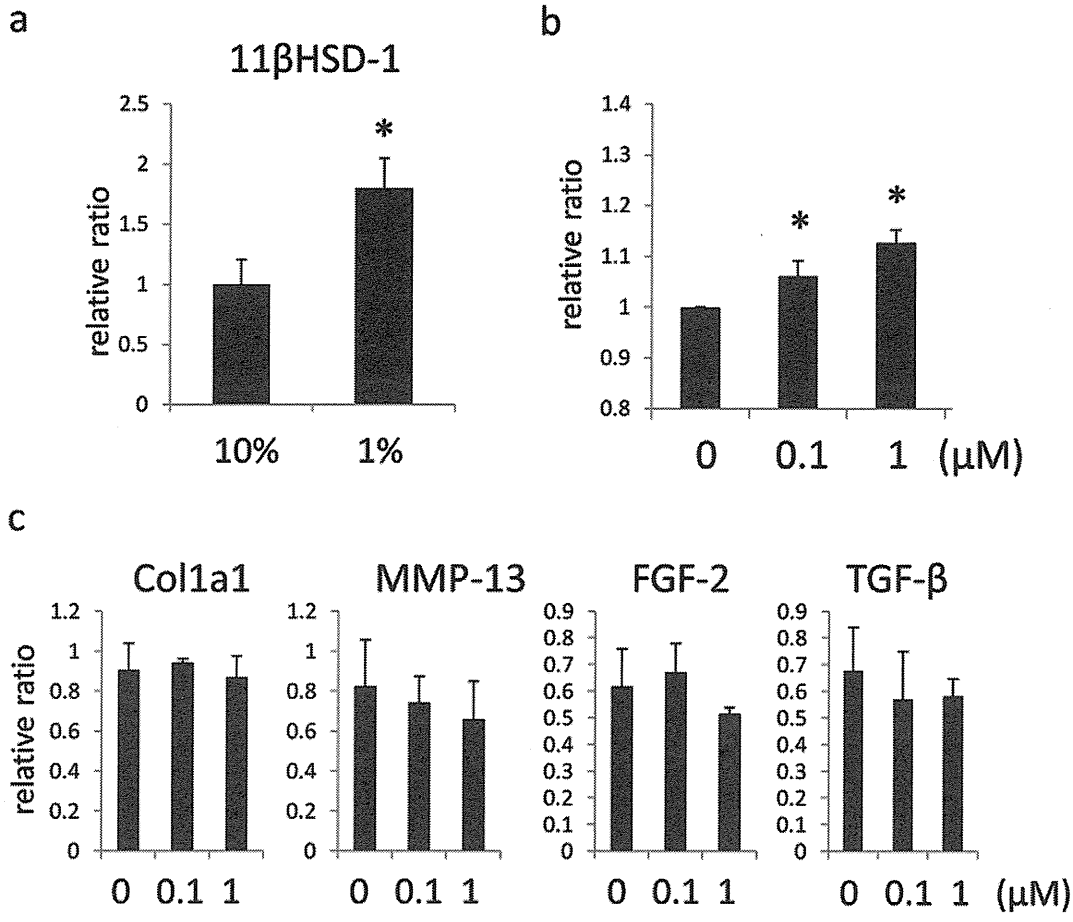

Figure 4. 11β-HSD1 regulates proliferation of NHDFs. (a) The relative expression of 11β-HSD1 in NDHF assessed by rtPCR with 10% FBS or 1% FBS in culture media. GAPDH was used as an internal control. (b) 11β-HSD1 selective inhibitor was applied to NHDFs cultured in DMEM containing 2% FBS at indicated dose and proliferation of the cells was assessed by MTS assay 72 h later. DMSO was applied as vehicle control. The histograms indicate means and SDs for eight independent experiments. An asterisk (*) indicates a statistically significant difference from the vehicle treated group ($P<0.05$, Student's *t*-test). (c) The relative expressions of Col1a1, MMP-1, FGF-2, TGF-β treated with 11β-HSD1 selective inhibitor at indicated dose for 48 h assessed by rtPCR. GAPDH was used as an internal control.
doi:10.1371/journal.pone.0025039.g004

not be used to evaluate the functions of 11β-HSD1 in cortisol production, proliferation, or differentiation of keratinocytes.

Next, we evaluated the effects of 11β-HSD1 inhibitor on the calcium-stimulated differentiation of NHEKs. Although calcium treatment increased the expression of 11β-HSD1, protein and mRNA for K1 or K10, and IVL were not affected by 1 to 10 μM of selective 11β-HSD1 inhibitor (Figure 3d,e). These results indicated that 11β-HSD1 might be involved in the proliferation but not in the differentiation of NHEKs.

11β-HSD1 regulates proliferation of NHDFs

We next investigated the function of 11β-HSD1 in NHDFs. Starving NHDFs by reducing medium concentrations of FBS from 10% to 1% for 24 h retards cell growth. The expression of 11β-HSD1 was significantly enhanced in starvation conditions (Figure 4a). Furthermore, similarly to the effects on keratinocytes, the selective 11β-HSD1 inhibitor at doses of 100 nM and 1 μM induced proliferation of NHDFs, demonstrating that 11β-HSD1 also negatively regulates NHDFs proliferation (Figure 4b). Next, the effect of 11β-HSD1 inhibitor on the expression of fibrogenic cytokines and fibroblast growth factors was evaluated (Figure 4c). However, inhibition of 11β-HSD1 at these doses did not affect the expression of Col1a1, MMP-13, TGF-β, or FGF-2. This indicates that 11β-HSD1 was not involved in collagen metabolism, and inhibits the proliferation of NHDFs via pathways independent of the autocrine effects of these cytokines and growth factors.

Topical application of 11β-HSD1 inhibitor induces hyperproliferation of the epidermis

To investigate the function of 11β-HSD1 *in vivo*, hairless mouse skin was exposed to 11β-HSD1 inhibitor. 11β-HSD1 is also expressed in the epidermis and fibroblasts of murine skin in C57BL/6 mice and Hos: HR-1 (hairless) mice (Figure 5a,b,d,e). The expression of 11β-HSD1 was also detected in cultured primary mouse keratinocytes and in cultured primary dermal fibroblasts derived from C57BL/6 and Hos: HR-1 mice (Figure 5c,f). Application of 50 μM selective 11β-HSD1 inhibitor to the dorsal skin of Hos: HR-1 mice for five continuous days induced acanthosis (Figure 5g). The epidermal thickness was significantly higher in selective 11β-HSD1 inhibitor treated groups than control groups (Figure 5h). In addition, the number of Ki-67 positive cells was significantly higher in 11β-HSD1 inhibitor treated skin than in vehicle treated skin (Figure 5i,j). These results demonstrate that 11β-HSD1 inhibitor also promotes the proliferation of keratinocytes *in vivo*.

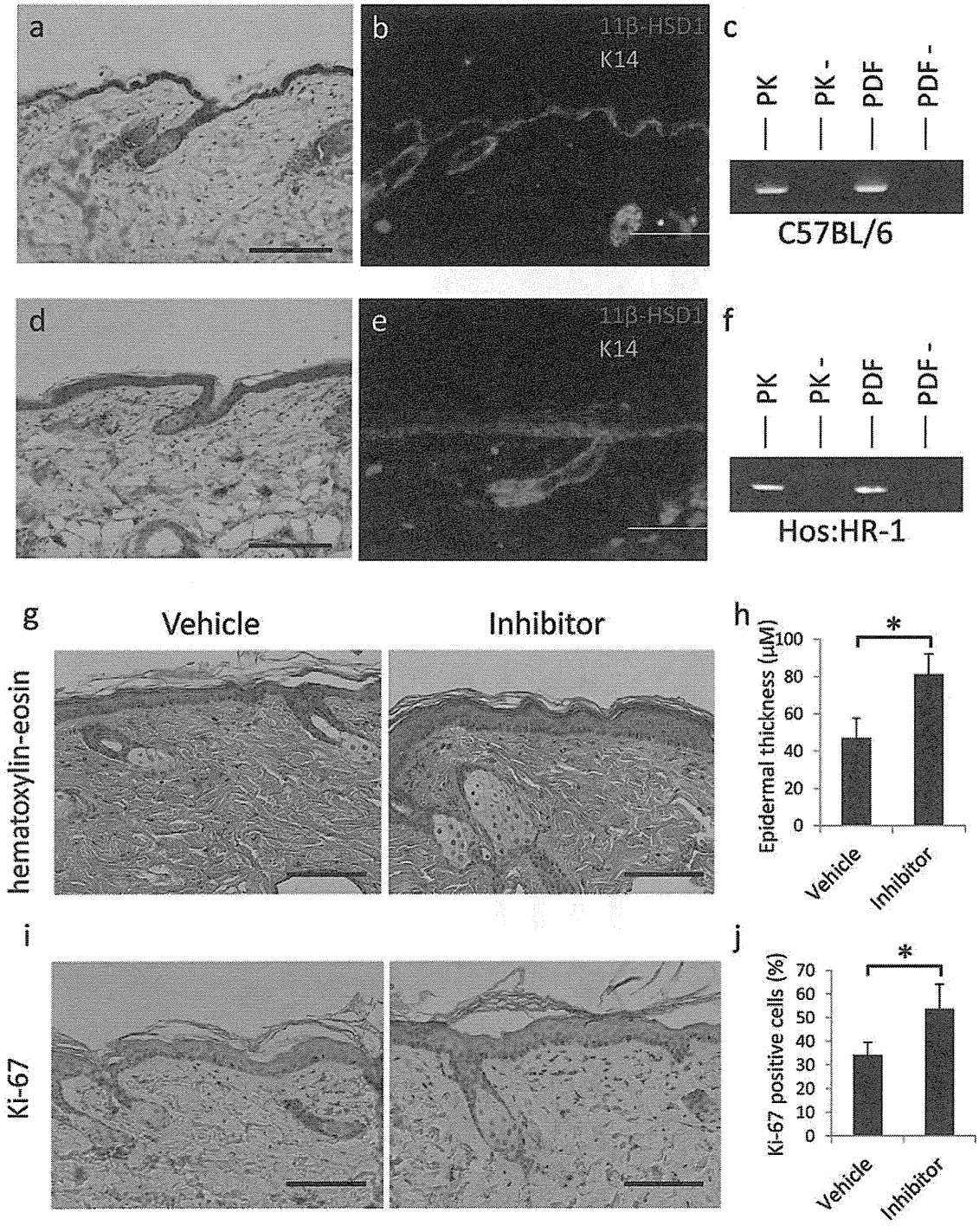

Figure 5. Selective inhibitor of 11β-HSD1 proliferates keratinocytes in murine skin. (a, d) Immunohistochemical staining of 11β-HSD1 (DAB staining) in C57BL/6 mouse (a) and Hos: HR-1 (hairless) mouse (d) skin tissue. Bar = 50 μM. (b, e) Immunofluorescent staining of 11β-HSD1 (red) and keratin 14 (green) in C57BL/6 mouse (b) and Hos: HR-1 mouse (e) skin tissue. Bar = 100 μM. (c, f) PCR detecting 11β-HSD1 in primary mouse keratinocytes and primary mouse dermal fibroblasts of C57BL/6 mouse (c) and Hos: HR-1 mouse (f). RT-: samples without reverse transcriptase (negative control). (g–j) Representative H&E staining (g) and Ki-67 staining (i) of 11β-HSD1 selective inhibitor or vehicle (1:1, acetone:olive oil) treated skin of Hos: HR-1 mice. Bar = 100 μm. (h) Epidermal thickness of vehicle and inhibitor treated mice. Intrafollicular epidermal thickness was calculated by averaging five locations in each section. Three sections from each mouse were evaluated. Bars show mean epidermal thickness ± SD of vehicle-treated mice (n = 5) and inhibitor-treated mice (n = 5; *P<0.01, Student's t-test). (j) The percentage of Ki-67 positive cells. Analyses were performed by counting the total number of basal cells and cells expressing nuclear Ki-67 stain. Three sections from each mouse were evaluated. Bars indicate mean ± SD of vehicle-treated mice (n = 5) and inhibitor-treated mice (n = 5; *P<0.05, Student's t-test).
doi:10.1371/journal.pone.0025039.g005

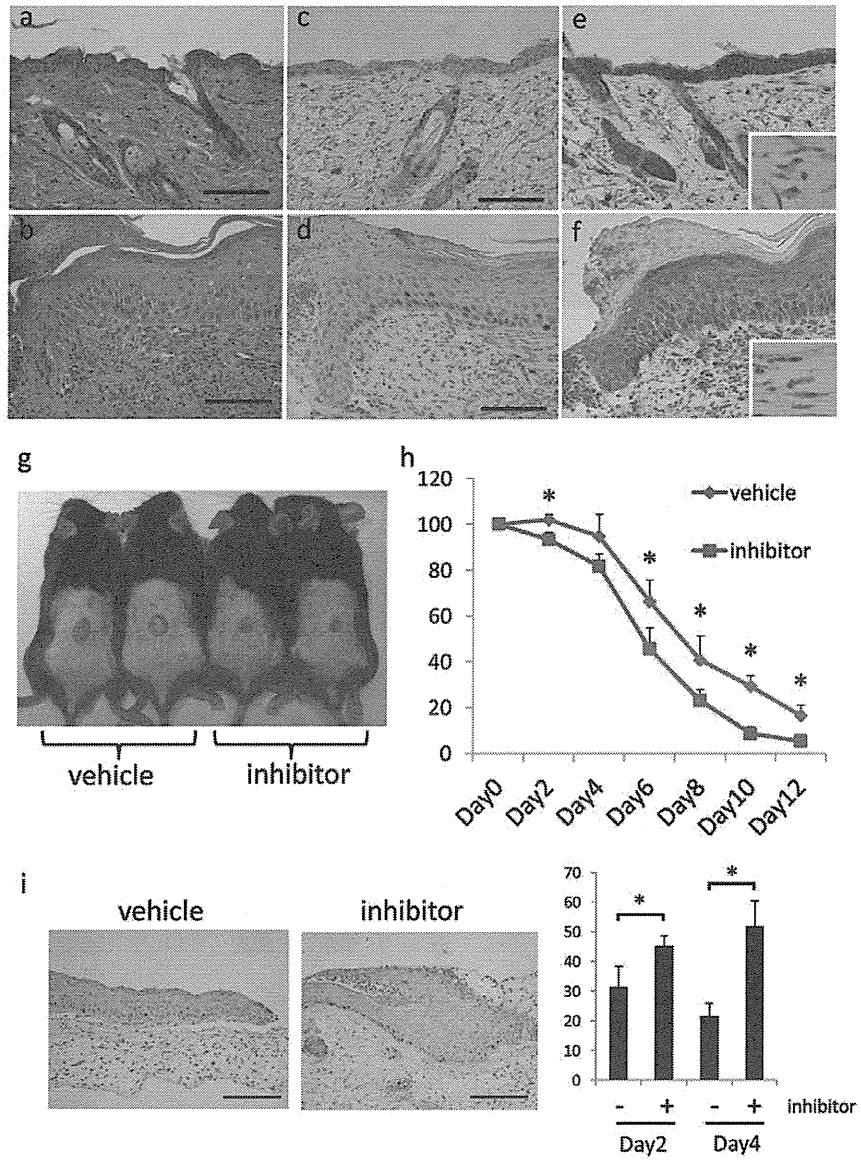

Figure 6. The role of 11β-HSD1 in wound healing of C57BL/6 mice. (a–f) H&E (a, b), Ki-67 (c, d), and 11β-HSD1 (e, f) staining of ulcer edge and non ulcer skin of the same section. Inserts: high magnification of the fibroblasts. Bar = 100 μm. (g) Macroscopic view of wound healing on day 10. A 15-mm wound was created on the back of 6-week-old male mice and wound closure was monitored with application of vehicle or 11β-HSD1 inhibitor every other day. (h) Reduction of wound area on days 2, 4, 6, 8, 10, and 12. The histograms indicate means and standard deviations for four mice in each group. An asterisk indicates a statistically significant difference (*$P<0.05$, Student's *t*-test). (i) Representative Ki-67 staining in day2 wound edge skin and the percentage of Ki-67 positive cells in day2 and day4 wound edge epidermis. Analyses were performed by counting the total number of basal cells and cells expressing nuclear Ki-67 stain. Bars indicate mean ± SD of vehicle-treated mice (n = 6) and inhibitor-treated mice (n = 6; *$P<0.05$, Student's *t*-test). Bar = 100 μm.
doi:10.1371/journal.pone.0025039.g006

11β-HSD1 inhibitor promotes wound healing in C57BL/6 mice

Taken together, these findings demonstrate that 11β-HSD1 regulates the proliferation of keratinocytes and fibroblasts. We therefore hypothesized that 11β-HSD1 inhibitor would promote wound healing. The keratinocytes at wound edges are hyperproliferative, thus the epidermis becomes thick in this region, with increased Ki-67 positive cells (Figure 6a–d). Interestingly, the intensity of 11β-HSD1 detected with immunohistochemical staining was lower in wound edge keratinocytes than in non wound keratinocytes in the same section (Figure 6e,f). The intensity of 11β-HSD1 did not differ between wound edge fibroblasts and non-wound fibroblasts (Figure 6e,f inserts). Because our data show that 11β-HSD1 negatively regulates the proliferation of keratinocytes, we considered that the decreased expression of 11β-HSD1 in wound edge keratinocytes might be promoting their proliferative state. To investigate whether selective 11β-HSD1 inhibitor could promote wound healing, we applied 10 μM 11β-HSD1 inhibitor every other day to wounds created on the dorsal skin of C57BL/6 mice. The wound areas were significantly smaller in the 11β-HSD1 inhibitor treated group than the vehicle treated group (Figure 6g,h). The number of Ki-67 positive cells was significantly higher on day2 and day4 wound edge epidermis in the 11β-HSD1 inhibitor treated group than the vehicle treated group (Figure 6i).

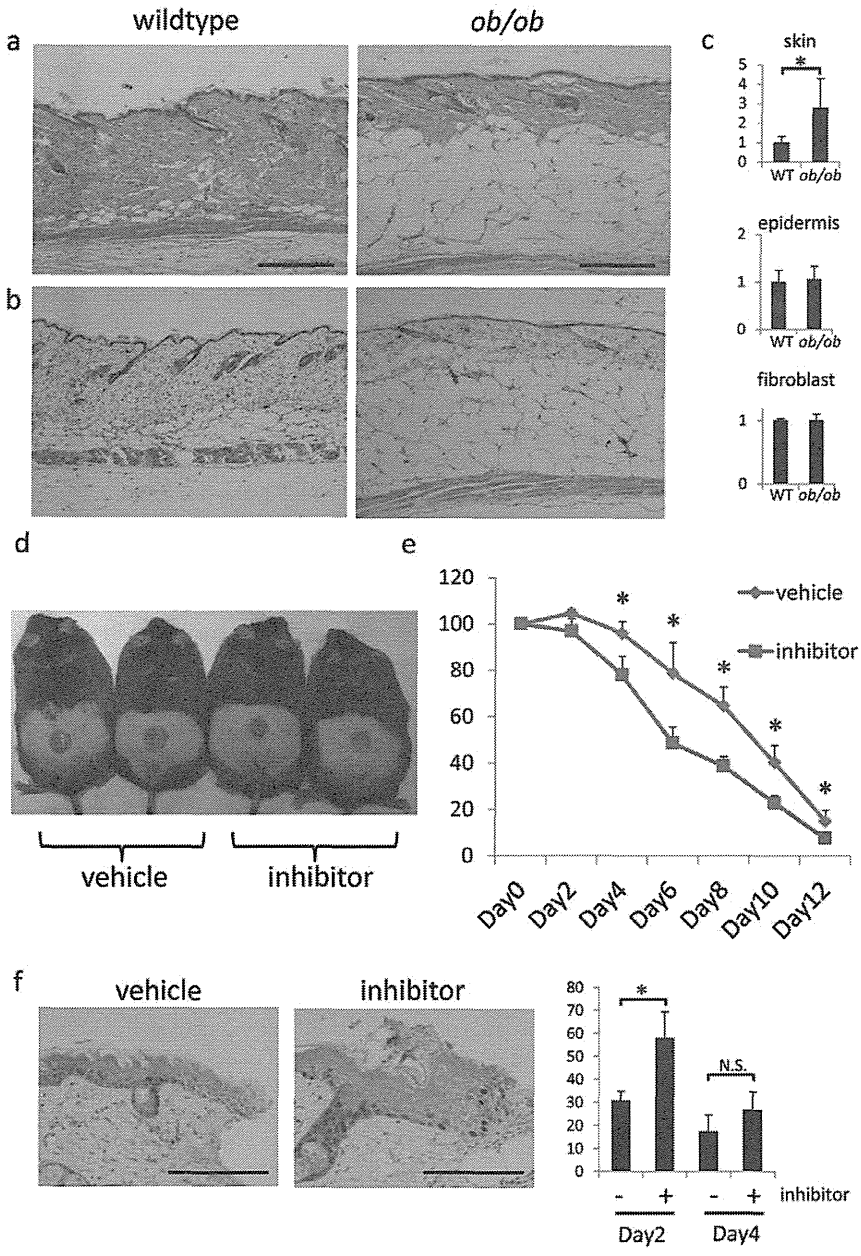

Figure 7. Selective 11β-HSD1 inhibitor enhance wound healing in *ob/ob* mice. (a,b) Representative H&E staining (a) and 11β-HSD1 staining (b) of 6-week-old male wildtype and *ob/ob* mice. Bar = 50 μm. (c) The relative expressions of 11β-HSD1 in epidermis, fibroblasts, and whole skin extract of wildtype and *ob/ob* mice assessed by rtPCR. GAPDH was used as an internal control ($P<0.05$, Student's *t*-test). (d) Macroscopic view of wound healing on day 8. A 15-mm wound was created on the back of 6-week-old male *ob/ob* mice and wound closure was monitored with application of vehicle or 11β-HSD1 inhibitor every other day. (e) Reduction of wound area on days 2, 4, 6, 8, 10, and 12. The histograms indicate means and standard deviations for four mice in each group. An asterisk indicates a statistically significant difference (*$P<0.05$, Student's *t*-test). (f) Representative Ki-67 staining in day4 wound edge skin and the percentage of Ki-67 positive cells in day2 and day4 wound edge epidermis. Analyses were performed by counting the total number of basal cells and cells expressing nuclear Ki-67 stain. Bars indicate mean ± SD of vehicle-treated mice (n = 3) and inhibitor-treated mice (n = 3; *$P<0.05$, Student's *t*-test). Bar = 100 μm.
doi:10.1371/journal.pone.0025039.g007

11β-HSD1 inhibitor promotes wound healing in *ob/ob* mice

We finally assessed wound healing in obese/obese (*ob/ob*) mice, the model of impaired wound healing. In *ob/ob* mice, the dermal layer was thinner, and the subcutaneous adipose layer was thicker, than in age-matched wildtype mice (Figure 7a). Interestingly, the expression of 11β-HSD1 was significantly higher in the skin extract of *ob/ob* mice, however, the expression did not differ in the epidermal extract and the fibroblast extract (Figure 7b,c). These data suggest that increased subcutaneous adipose tissue in *ob/ob* mice is responsible for increased expression of 11β-HSD1 in the skin extract. Notably, application of 10 μM 11β-HSD1 inhibitor every other day improved wound healing more in *ob/ob* mice than in C57BL/6 mice (Figure 7d and 7e). The number of Ki-67 positive cells was significantly higher on day2 wound edge epidermis in the 11β-HSD1 inhibitor treated group than the vehicle treated group (Figure 7f).

Discussion

The present study shows that 11β-HSD1 is a regulator of keratinocyte and fibroblast proliferation. We found that the expression of 11β-HSD1 is higher in the cytoplasm of supra-basal differentiating cells than in basal proliferating cells of the normal epidermis, and that the inhibition of 11β-HSD1 increases the proliferation of keratinocytes and fibroblasts. We also report that topical application of a selective 11β-HSD1 inhibitor promotes keratinocyte proliferation and wound healing.

Skin is one of the most chronically stress-loaded tissues because it faces the outside environment and is exposed to stressors including bacteria, ultraviolet radiation, and mechanical stimulation. Thus, it makes intuitive sense that skin expresses the functional cortisol activating enzyme 11β-HSD1. Specifically, our experiments using immunofluorescence staining revealed that 11β-HSD1 is expressed in the supra-basal area of the epidermis. This expression pattern of 11β-HSD1 is different from previous reports [17]. However, 11β-HSD1 expression being limited to the supra-basal epidermal area seems reasonable, considering that 11β-HSD1-mediated suppression of excessive proliferation in differentiated keratinocytes might contribute to maintain adequate epidermal thickness. In addition to its known anti-inflammatory properties, glucocorticoid (e.g., cortisol and corticosterone) is known to regulate the proliferation of keratinocytes and prolong epidermal turnover time [22,23,24,25]. Consistent with this, we have shown that selective inhibition of 11β-HSD1 promotes the proliferation of keratinocytes both *in vitro* and *in vivo*, suggesting that intracellular activators of cortisol would negatively regulate keratinocyte proliferation (Figure 3 and 5). Hence, we conclude that topical application of selective 11β-HSD1 inhibitor has the potential to be an effective treatment to stimulate the proliferation of keratinocytes. However, we observed that high doses of selective 11β-HSD1 inhibitor and siRNA knock down of 11β-HSD1 decreased the viability of keratinocytes. Thus, it is important to determine the optimal dosage to stimulate proliferation without unwanted toxic effects. Unexpectedly, the selective 11β-HSD1 inhibitor did not influence calcium-induced differentiation of keratinocytes. As calcium-induced differentiation *in vitro* differs from *in vivo* differentiation, further study may needed to determine if 11β-HSD1 plays a functional role in keratinocyte differentiation.

Glucocorticoids are known to increase in response to stress or medical therapy, and impair wound healing because they inhibit proliferation of cells and proinflammatory cytokine production [26,27]. In this study, we showed that 11β-HSD1 inhibitor significantly promotes cutaneous wound healing. We think the decrease in the expression of 11β-HSD1 in keratinocytes at wound edges might be a normal physiological mechanism that promotes the proliferation of keratinocytes during wound healing. Thus, the selective 11β-HSD1 inhibitor might promote wound healing because it supports this mechanism. The selective 11β-HSD1 inhibitor also promotes the proliferation of NHDFs *in vitro*, and the effect of the inhibitor on fibroblasts also might assist wound healing. The effect of inhibitor on endothelial cells and inflammatory cytokines, which also are important factors in wound healing, needs to be evaluated in the future.

It is intriguing that the inhibitor has a stronger effect on wound healing in *ob/ob* mice, a model of impaired wound healing. These mice exhibit severe diabetes and obesity syndromes, phenotypes mediated by the loss of the ob gene product: the 16 kDa cytokine leptin [28,29]. The expression of 11β-HSD1 is elevated in stromal vascular cells and mature adipocytes isolated from the adipose tissue of *ob/ob* mice [30]. Interestingly, the expression of 11β-HSD1 was also elevated in the skin extract of *ob/ob* mice (Figure 7c). The selective 11β-HSD1 inhibitor promoted wound healing in *ob/ob* mice, almost to the same level as the inhibitor treated group of C57BL/6 mice. Thus, we hypothesize that increased expression of 11β-HSD1 in *ob/ob* mouse skin might play an important role in delayed wound healing in *ob/ob* mice. The mouse skin extract is composed of epidermis, dermis, subcutaneous adipose tissue, and cutaneous muscular tissue. It was recently reported that subcutaneous adipose tissue is an important regulator of dermal fibroblast proliferation in high-fat diet induced obese mice [31]. It is possible that not only keratinocytes and fibroblasts, but also the subcutaneous adipose layer, which is markedly increased in *ob/ob* mice, could be a source of 11β-HSD1 in *ob/ob* mice as the expression of 11β-HSD1 did not differ in the epidermal extract and the fibroblast extract. We think that the 11β-HSD1 inhibitor might also act on the subcutaneous adipose tissue to accelerate wound healing in *ob/ob* mice, although further study is needed to test this theory.

Obesity is a global problem that affects 400 million adults worldwide [12,32]. Adipose tissue overexpression of 11β-HSD1 is observed in human obesity, and inhibition of 11β-HSD1 has been proposed to be of potential therapeutic benefit to patients with obesity and type 2 diabetes mellitus [33,34,35]. Our results suggest that in addition to systemic administration of 11β-HSD1 inhibitor, topical application of 11β-HSD1 inhibitor is potentially effective for the treatment of the chronic wounds of obese and diabetic patients.

In summary, the present study identifies a novel role for 11β-HSD1 in the promotions of keratinocyte and fibroblast proliferation. Targeting 11β-HSD1 could be a novel approach to treat chronic wounds, and skin diseases with aberrant proliferation.

Author Contributions

Conceived and designed the experiments: MT HM EM IK. Performed the experiments: MT KI A. Kimura A. Kato AI. Analyzed the data: MT A. Kimura. Contributed reagents/materials/analysis tools: MT. Wrote the paper: MT.

References

1. Sapolsky RM, Romero LM, Munck AU (2000) How do glucocorticoids influence stress responses? Integrating permissive, suppressive, stimulatory, and preparative actions. Endocr Rev 21: 55–89.
2. Zhou J, Cidlowski JA (2005) The human glucocorticoid receptor: one gene, multiple proteins and diverse responses. Steroids 70: 407–417.
3. Revollo JR, Cidlowski JA (2009) Mechanisms generating diversity in glucocorticoid receptor signaling. Ann N Y Acad Sci 1179: 167–178.
4. Adcock IM, Caramori G (2001) Cross-talk between pro-inflammatory transcription factors and glucocorticoids. Immunol Cell Biol 79: 376–384.
5. Stojadinovic O, Lee B, Vouthounis C, Vukelic S, Pastar I, et al. (2007) Novel genomic effects of glucocorticoids in epidermal keratinocytes: inhibition of apoptosis, interferon-gamma pathway, and wound healing along with promotion of terminal differentiation. J Biol Chem 282: 4021–4034.
6. Seckl JR, Walker BR (2001) Minireview: 11beta-hydroxysteroid dehydrogenase type 1- a tissue-specific amplifier of glucocorticoid action. Endocrinology 142: 1371–1376.
7. Sandeep TC, Walker BR (2001) Pathophysiology of modulation of local glucocorticoid levels by 11beta-hydroxysteroid dehydrogenases. Trends Endocrinol Metab 12: 446–453.
8. Ishii T, Masuzaki H, Tanaka T, Arai N, Yasue S, et al. (2007) Augmentation of 11beta-hydroxysteroid dehydrogenase type 1 in LPS-activated J774.1 macrophages–role of 11beta-HSD1 in pro-inflammatory properties in macrophages. FEBS Lett 581: 349–354.
9. Odermatt A, Atanasov AG, Balazs Z, Schweizer RA, Nashev LG, et al. (2006) Why is 11beta-hydroxysteroid dehydrogenase type 1 facing the endoplasmic reticulum lumen? Physiological relevance of the membrane topology of 11beta-HSD1. Mol Cell Endocrinol 248: 15–23.
10. Desbriere R, Vuaroqueaux V, Achard V, Boullu-Ciocca S, Labuhn M, et al. (2006) 11beta-hydroxysteroid dehydrogenase type 1 mRNA is increased in both visceral and subcutaneous adipose tissue of obese patients. Obesity (Silver Spring) 14: 794–798.
11. Mericq V, Medina P, Bouwman C, Johnson MC, Godoy J, et al. (2009) Expression and activity of 11beta-hydroxysteroid dehydrogenase type 1 enzyme

in subcutaneous and visceral adipose tissue of prepubertal children. Horm Res 71: 89–93.
12. Morton NM (2010) Obesity and corticosteroids: 11beta-hydroxysteroid type 1 as a cause and therapeutic target in metabolic disease. Mol Cell Endocrinol 316: 154–164.
13. Masuzaki H, Paterson J, Shinyama H, Morton NM, Mullins JJ, et al. (2001) A transgenic model of visceral obesity and the metabolic syndrome. Science 294: 2166–2170.
14. Masuzaki H, Yamamoto H, Kenyon CJ, Elmquist JK, Morton NM, et al. (2003) Transgenic amplification of glucocorticoid action in adipose tissue causes high blood pressure in mice. J Clin Invest 112: 83–90.
15. Tiganescu A, Walker EA, Hardy RS, Mayes AE, Stewart PM (2011) Localization, Age- and Site-Dependent Expression, and Regulation of 11beta-Hydroxysteroid Dehydrogenase Type 1 in Skin. J Invest Dermatol.
16. Hennebert O, Chalbot S, Alran S, Morfin R (2007) Dehydroepiandrosterone 7alpha-hydroxylation in human tissues: possible interference with type 1 11beta-hydroxysteroid dehydrogenase-mediated processes. J Steroid Biochem Mol Biol 104: 326–333.
17. Cirillo N, Prime SS (2011) Keratinocytes synthesize and activate cortisol: first characterisation of a novel epidermal glucocorticoid system. J Cell Biochem;in press.
18. Terao M, Murota H, Kitaba S, Katayama I (2010) Tumor necrosis factor-alpha processing inhibitor-1 inhibits skin fibrosis in a bleomycin-induced murine model of scleroderma. Exp Dermatol 19: 38–43.
19. Hermanowski-Vosatka A, Balkovec JM, Cheng K, Chen HY, Hernandez M, et al. (2005) 11beta-HSD1 inhibition ameliorates metabolic syndrome and prevents progression of atherosclerosis in mice. J Exp Med 202: 517–527.
20. Micallef L, Belaubre F, Pinon A, Jayat-Vignoles C, Delage C, et al. (2009) Effects of extracellular calcium on the growth-differentiation switch in immortalized keratinocyte HaCaT cells compared with normal human keratinocytes. Exp Dermatol 18: 143–151.
21. Bikle DD, Oda Y, Xie Z (2004) Calcium and 1,25(OH)2D: interacting drivers of epidermal differentiation. J Steroid Biochem Mol Biol 89–90: 355–360.
22. Choi EH, Demerjian M, Crumrine D, Brown BE, Mauro T, et al. (2006) Glucocorticoid blockade reverses psychological stress-induced abnormalities in epidermal structure and function. Am J Physiol Regul Integr Comp Physiol 291: R1657–1662.
23. Sheu HM, Tai CL, Kuo KW, Yu HS, Chai CY (1991) Modulation of epidermal terminal differentiation in patients after long-term topical corticosteroids. J Dermatol 18: 454–464.
24. Zoller NN, Kippenberger S, Thaci D, Mewes K, Spiegel M, et al. (2008) Evaluation of beneficial and adverse effects of glucocorticoids on a newly developed full-thickness skin model. Toxicol In Vitro 22: 747–759.
25. Demerjian M, Choi EH, Man MQ, Chang S, Elias PM, et al. (2009) Activators of PPARs and LXR decrease the adverse effects of exogenous glucocorticoids on the epidermis. Exp Dermatol 18: 643–649.
26. Hubner G, Brauchle M, Smola H, Madlener M, Fassler R, et al. (1996) Differential regulation of pro-inflammatory cytokines during wound healing in normal and glucocorticoid-treated mice. Cytokine 8: 548–556.
27. Christian LM, Graham JE, Padgett DA, Glaser R, Kiecolt-Glaser JK (2006) Stress and wound healing. Neuroimmunomodulation 13: 337–346.
28. Coleman DL (1978) Obese and diabetes: two mutant genes causing diabetes-obesity syndromes in mice. Diabetologia 14: 141–148.
29. Zhang Y, Proenca R, Maffei M, Barone M, Leopold L, et al. (1994) Positional cloning of the mouse obese gene and its human homologue. Nature 372: 425–432.
30. Ishii-Yonemoto T, Masuzaki H, Yasue S, Okada S, Kozuka C, et al. (2010) Glucocorticoid reamplification within cells intensifies NF-kappaB and MAPK signaling and reinforces inflammation in activated preadipocytes. Am J Physiol Endocrinol Metab 298: E930–940.
31. Ezure T, Amano S (2010) Increased subcutaneous adipose tissue impairs dermal function in diet-induced obese mice. Exp Dermatol 19: 878–882.
32. Rigby NJ, Kumanyika S, James WP (2004) Confronting the epidemic: the need for global solutions. J Public Health Policy 25: 418–434.
33. Bujalska IJ, Gathercole LL, Tomlinson JW, Darimont C, Ermolieff J, et al. (2008) A novel selective 11beta-hydroxysteroid dehydrogenase type 1 inhibitor prevents human adipogenesis. J Endocrinol 197: 297–307.
34. Hollis G, Huber R (2011) 11beta-Hydroxysteroid dehydrogenase type 1 inhibition in type 2 diabetes mellitus. Diabetes Obes Metab 13: 1–6.
35. Hale C, Wang M (2008) Development of 11beta-HSD1 inhibitors for the treatment of type 2 diabetes. Mini Rev Med Chem 8: 702–710.

Allergology International. 2012;61:469-473
DOI: 10.2332/allergolint.12-OA-0429

ORIGINAL ARTICLE

Abnormal Axon Reflex-Mediated Sweating Correlates with High State of Anxiety in Atopic Dermatitis

Akiko Kijima[1], Hiroyuki Murota[1], Saki Matsui[1], Aya Takahashi[1], Akihiro Kimura[1], Shun Kitaba[1], Jeong-Beom Lee[2] and Ichiro Katayama[1]

ABSTRACT

Background: Sweating plays a key role in skin homeostasis, including antimicrobial and moisturizing effects, and regulation of skin surface pH. Impaired axon reflex-mediated (AXR) sweating has been observed in patients with atopic dermatitis (AD). However, the mechanism of such abnormal sudomotor axon reflex remains to be revealed.

Methods: To investigate this mechanism, sudomotor function was analyzed using a quantitative sudomotor axon reflex test (acetylcholine iontophoresis) in patients with AD (n = 26) and healthy volunteers (n = 12). Correlation between sudomotor function and certain background factors, including Spielberger State Trait Anxiety Inventory score, Severity Scoring of Atopic Dermatitis (SCORAD) score, number of circulating eosinophils, and serum concentrations of thymus and activation-regulated chemokine and immunoglobulin E radioimmunosorbent test, was validated.

Results: Latency time was significantly prolonged in AD (p = 0.0352), and AXR sweating volume (mg/0-5 min) was significantly lower in AD patients than in healthy controls (p = 0.0441). Direct sweating volume (mg/0-5 min) was comparable in AD patients and healthy controls. A significant correlation between the evaluation results of quantitative sudomotor axon reflex tests and certain background factors was not observed. The latency time in non-lesioned and lesioned areas for AD patients versus continuous anxiety value in the Spielberger State Trait Anxiety Inventory and the AXR versus SCORAD showed significant correlations (p = 0.0424, p = 0.0169, and p = 0.0523, respectively).

Conclusions: Although the number of study subjects was little, abnormal AXR sweating in patients with AD was observed. Correlative analysis suggests possible involvement of continuous anxiety and the immune system in such abnormal sudomotor function.

KEY WORDS

acetylcholine, anxiety, atopic dermatitis, axon reflex, sweating

INTRODUCTION

Sweating plays a key role in skin homeostasis, with antimicrobial[1,2] and moisturizing effects,[3] and in the regulation of skin surface pH.[4] Certain data also suggest that impaired sweating contributes to the pathogenesis of atopic dermatitis (AD). It has been reported that showering at school reduces the severity of AD.[5] Since it is known that the pHs of both sweat and the skin surface increase with time,[6] old sweat might cause skin barrier dysfunction and promote infection, which are regarded as exacerbating factors for AD.[4,7] In contrast, decreased sweating might cause dry skin and exacerbate skin symptoms in AD. In fact, acetylcholine (ACh)-mediated sweating is impaired in patients with AD.[3] Furthermore, a significant increase in ACh tissue content[8] and reduced ACh receptor expression levels[9] in lesioned skin of AD patients suggest that the cholinergic system of the skin is modulated in AD. This belief assumes that

[1]Department of Dermatology, Course of Integrated Medicine, Graduate School of Medicine, Osaka University, Osaka, Japan and [2]Department of Physiology, College of Medicine, Soonchunhyang University, Chenan, Republic of Korea.
Conflict of interest: The authors have no conflict of interest.
Correspondence: Hiroyuki Murota, Department of Dermatology, Course of Integrated Medicine, Graduate School of Medicine, Osaka University, 2-2 Yamadaoka, Suita, Osaka 565-0871, Japan.
Email: h-murota@derma.med.osaka-u.ac.jp
Received 23 January 2012. Accepted for publication 19 March 2012.

a modulated ACh system might affect sudation in AD; however, ACh-induced direct sweat volume does not appear to be affected.[3] Looking at an altered ACh system in the local skin alone cannot explain abnormal sweating responses in AD patients.

To assess the reproducibility of sudomotor function in AD patients, a quantitative sudomotor axon reflex test (QSART)[10] was performed. To elucidate the mechanisms of altered ACh-induced sweating, we evaluated the correlation between the measurements of sweating and certain clinical factors, including Spielberger State Trait Anxiety Inventory (STAI) score, serum concentrations of immunoglobulin E radioimmunosorbent test (IgE-RIST) and thymus and activation-regulated chemokine (TARC), and the number of circulating eosinophils.

METHODS

SUBJECTS

Quantitative Sudomotor Axon Reflex Test (QSART)

Examination was performed based on the method established by Lee *et al.*.[10] Briefly, the subjects were asked to remain quiet for 60 min before undergoing QSART in a hospital outpatient clinic at constant temperature (20℃) and humidity (60%). The multicompartmental sweat capsule used in QSART consists of two independent compartments (Fig. 1A). ACh (100 mg/ml) iontophoretically applied to the skin from the outer compartment stimulates the underlying sweat glands directly (DIR sweating), while the glands of the skin in the central compartment of the capsule are activated indirectly via an axon reflex (AXR sweating; Fig. 1B-D). The central compartment of the capsule serves as the site for AXR sweat volume measurement during the 5 min of iontophoresis. Data for DIR sweating were obtained over the subsequent 5 min.

Sweat onset time, that is, the latency period for sweating after current loading (latency time), and sweat volume over 5 min were measured, and the area under the sweating curve was calculated from 0-5 min for AXR sweating and from 6-11 min for DIR sweating. As for the measurement of DIR sweating volume, a few cases with immeasurable volumes were omitted from the Table 1.

Study Design

This study was approved by the Institutional Review Board of Osaka University Hospital. Measurements of serum TARC and total IgE (radioimmunoassay) concentrations and eosinophil number were performed on all study subjects after they signed an informed consent form and provided written and oral information to the study physicians. Patients with AD fulfilled diagnostic criteria by both Hanifin and Rajka [11] and the Japanese Dermatological Association.[12] As a result, 26 adult patients with AD [male : female; 11 : 15, 43.58 ± 15.3 years old; mean ± standard deviation (SD)] and 12 healthy volunteers (male : female; 5 : 7, 32 ± 5.8 years old; mean ± SD) were admitted into the study. The severity of AD was assessed with Severity Scoring of Atopic Dermatitis (SCORAD).[13] STAI, designed and standardized by Spielberger *et al.*, was used to evaluate anxiety.[14]

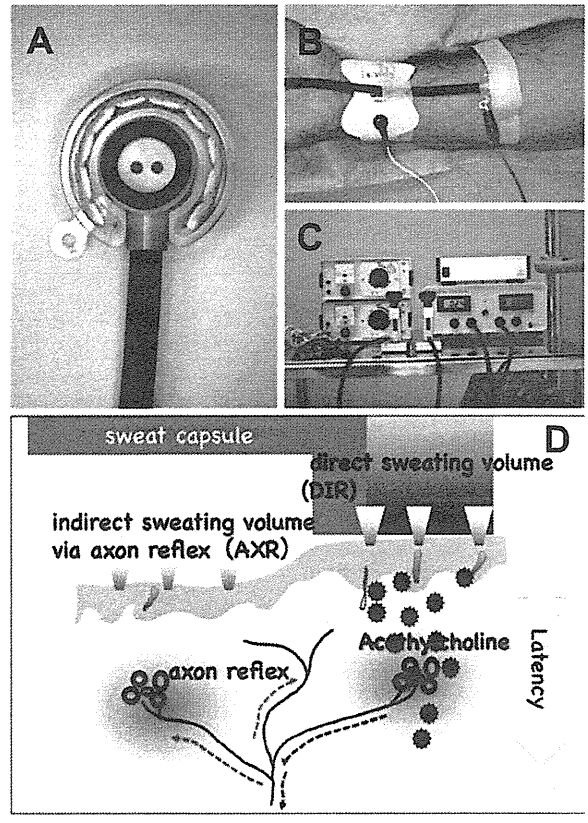

Fig. 1 Equipment and procedures for QSART. (**A**) The measurement sensor for sweating volume (sweat capsule: middle compartment) is surrounded by the outer compartment with a sponge-like device for iontophoresis. (**B**) Example of how the sweat capsule is used. Electrode for iontophoresis is placed on the wrist. (**C**) Sweat volume-measuring machine (lower right, SKINOS SKD-2000, Nagano, Japan), digital analyzer of measured sweat volume (upper right), and power source of iontophoresis (left). (**D**) Illustration of QSART.

Laboratory Methods

Fasting blood samples were drawn from the subjects. After serum separation, levels of TARC and IgE and eosinophil number were measured by enzyme-linked immunosorbent assay, radioimmunoassay, and visual evaluation, respectively.

Table 1 Correlation between clinical data and altered sudomotor function

		STAI (trait anxiety)	STAI (state anxiety)	SCORAD	TARC	IgE-RIST	Eosinophil	Age
Latency	NL	$n = 26$ $r = 0.4266$ $p = 0.0424$	$n = 26$ r = 0.3628 $p = 0.0970$	$n = 26$ r = -0.1736 $p = 0.3964$	$n = 26$ r = -0.2252 $p = 0.2790$	$n = 26$ r = 0.03887 $p = 0.8537$	$n = 26$ r = -0.04125 $p = 0.8414$	$n = 26$ r = 0.1529 $p = 0.4655$
	L	$n = 26$ $r = 0.5273$ $p = 0.0169$	$n = 26$ r = -0.05509 $p = 0.8028$	$n = 26$ r = 0.04284 $p = 0.8389$	$n = 26$ r = -0.03478 $p = 0.8718$	$n = 26$ r = 0.3256 $p = 0.1123$	$n = 26$ r = -0.02849 $p = 0.8901$	$n = 26$ r = -0.0805 $p = 0.7022$
AXR	NL	$n = 26$ r = -0.3114 $p = 0.1481$	$n = 26$ r = -0.1381 $p = 0.5298$	$n = 26$ r = 0.4575 $p = 0.0099$	$n = 26$ r = 0.2010 $p = 0.3248$	$n = 26$ r = -0.01775 $p = 0.9314$	$n = 26$ r = -0.2664 $p = 0.1883$	$n = 26$ r = -0.1249 $p = 0.5520$
	L	$n = 26$ r = 0.08509 $p = 0.6995$	$n = 26$ r = -0.07144 $p = 0.7520$	$n = 26$ r = 0.02314 $p = 0.9107$	$n = 26$ r = 0.1096 $p = 0.5939$	$n = 26$ r = 0.04424 $p = 0.8301$	$n = 26$ r = 0.05705 $p = 0.7774$	$n = 26$ r = -0.07954 $p = 0.7055$
DIR	NL	$n = 21$ r = -0.04935 $p = 0.8508$	$n = 21$ r = 0.08784 $p = 0.7374$	$n = 21$ r = 0.1272 $p = 0.5826$	$n = 21$ r = -0.09078 $p = 0.6956$	$n = 21$ r = 0.2742 $p = 0.2291$	$n = 21$ r = -0.007898 $p = 0.9708$	$n = 26$ r = -0.1006 $p = 0.6324$
	L	$n = 21$ r = 0.2880 $p = 0.2624$	$n = 21$ r = 0.2293 $p = 0.3759$	$n = 21$ r = -0.2654 $p = 0.2449$	$n = 21$ r = 0.1043 $p = 0.6440$	$n = 21$ r = 0.1299 $p = 0.5646$	$n = 21$ r = 0.1289 $p = 0.5393$	$n = 26$ r = 0.1781 $p = 0.3943$

NL, non-lesional; L, lesional.

Case number (n), Pearson r (r), and p value (two-tailed) (p).

RESULTS

ACh-INDUCED SWEATING VOLUME IN HEALTHY AND AD SUBJECTS

ACh-induced DIR and AXR mediated sweating volume were measured in healthy and AD subjects. First, comparison of AXR or DIR-mediated sweating volume between healthy and AD subjects (non-lesioned area) was performed (Fig. 2A). AXR-mediated sweating volume in AD patients (non-lesioned area) was significantly lower than that in healthy subjects. On the one hand, DIR-mediated sweating volume in AD patients was comparable to that of healthy subjects (Fig. 2A). Next, comparison between lesioned and non-lesioned skin in subjects with AD was performed (Fig. 2B). AXR-mediated sweating volume in lesioned skin was significantly lower than that in non-lesioned skin. These results indicate that AXR-, but not DIR-mediated sweating, is attenuated in AD subjects (Fig. 2C).

LATENCY TIME FOR ACh-INDUCED SWEATING IN HEALTHY AND AD SUBJECTS

Time to onset of sweating after the start of ACh iontophoresis (latency time) was measured (Fig. 3). Latency time in subjects with AD (non-lesioned skin) was significantly prolonged compared with healthy subjects ($p = 0.0352$, unpaired t test) (Fig. 3A). Unexpectedly, there was no difference between non-lesioned and lesioned skin in AD subjects (Fig. 3B), suggesting that abnormal ACh-induced sweating responses are commonly found in AD subjects regardless of the presence or absence of dermatitis.

RELATED BACKGROUND FACTORS TO ALTERED SUDOMOTOR FUNCTION

To explore the mechanisms of abnormal ACh-induced sweating in AD subjects, the relationships between measurements of sweating and certain clinical factors, such as the STAI score, SCORAD score, number of circulating eosinophils, and serum concentrations of TARC and IgE-RIST, were verified. As shown in the Table 1, trait anxiety vs. latency time (both non-lesioned and lesioned skin) and SCORAD vs. AXR-mediated sweating volume in non-lesioned skin showed significant positive correlations. Other parameters did not have a significant correlation with measurements of sweating.

DISCUSSION

The involvement of sweating in the pathogenesis of AD has become a major topic of discussion. As mentioned above, recent studies have organized the pathogenic involvement of sweat to include not only a barrier function but also the exacerbation of AD.[1,3,5,9] However, the cause and mechanism of abnormal ACh-induced axon reflex sweating in AD patients remain unclear.[3] Here, we validated the reproducibility of QSART in AD subjects. As a result, decreased axon reflex-mediated sweating volume and prolonged latency time in subjects with AD were confirmed. It was noteworthy that these findings were also observed in non-lesioned skin of AD patients. This phenomenon implies that local inflammation alone cannot explain the impaired sudomotor function in AD. Although there is no direct evidence supporting this

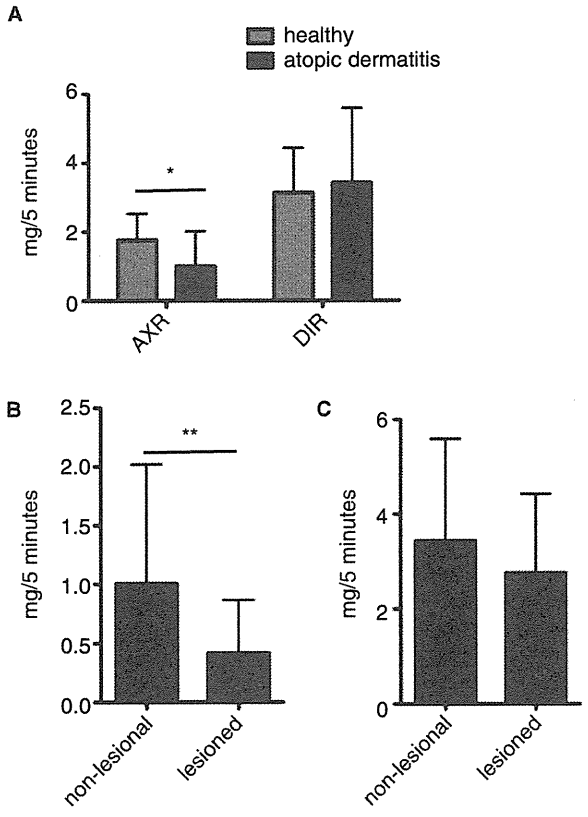

Fig. 2 Measurements of ACh-induced sweating volume in healthy and AD subjects. (**A**) AXR- and DIR-related sweating volume in healthy volunteers (gray) and non-lesioned areas of AD patients (black). *$p < 0.05$, unpaired t test. (**B**) Comparison of AXR-mediated sweating volume between non-lesioned and lesioned skin in patients with AD. **$p < 0.01$, paired t test. (**C**) Comparison of DIR-mediated sweating volume between non-lesioned and lesioned skin in patients with AD.

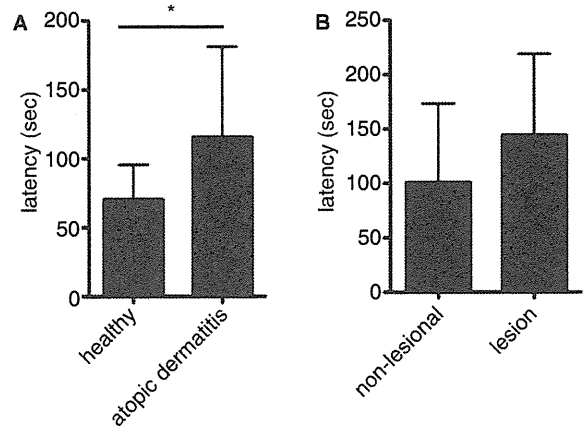

Fig. 3 Examination outcomes for latency time of ACh-induced sweating in healthy and AD subjects. (**A**) Comparisons of latency time between non-lesioned and lesioned skin in patients with AD. *$p < 0.05$, paired t test. (**B**) Comparisons of latency time between non-lesioned and lesioned skin in patients with AD.

hypothesis, ACh has been reported to accumulate in lesioned skin in AD patients.[8] Thus, it might be supposed that ACh receptor down-regulation in the skin of those with AD might occur via ACh saturation. To explore the cause of this abnormity, this report focused on certain clinical parameters.

Interestingly, trait anxiety was positively correlated to latency time in both non-lesioned and lesioned areas of AD. Although, there was few evidence supporting the relationship between trait anxiety and ACh, Sklan *et al.* reported that the higher the trait anxiety, the lower the enzyme activity of acethylcholinesterase (AChE).[15] Furthermore, previous studies had suggested that AD is a skin disease associated with increased anxiety levels.[16,17] Though this might be just a mere coincidence, if enzymatic activity of AChE decreased in AD, the dysregulation might cause the anxious mood and the accumulation of ACh, confirming past findings.[8,16,17] Thus, the enzymatic activity of AChE in AD was considered worthy of attention. In a measurement of sweat volume, despite marked reduction in AXR-mediated sweating volume in AD subjects, DIR-mediated sweating volume was preserved. Therefore, it could be proposed that malfunction of sudomotor nerve might lead to decrease in the AXR-mediated sweating response in AD (Fig. 4). Such an anomaly in the sweating response in AD patients might lead to the development of dry skin (Fig. 4).

The other positive correlation was found between SCORAD and AXR-mediated sweating volume in non-lesioned areas (Table 1). It is difficult to explain why these factors correlate with each other, despite no definite correlation between SCORAD and AXR-mediated sweating volume in lesioned areas. However, we treated increased AXR-mediated sweating volume in non-lesioned area the same as in cases of compensatory hyperhidrosis, which is occasionally observed in cases of invasive treatments of hyperhidrosis.[18] Thus, it might be speculated that damaged sympathetic nerves in lesioned skin had relatively increased the sweating volume in surrounding non-lesioned areas.

Regarding the correlation between SCORAD and trait or state anxiety level, there was no correlation (data not shown), similar to the previous report.[17] This result led us to think that high anxiety level was not just result of disease severity. Yet, in this study, there were limitations in the statistical strategy that had assessed the relation between a variety of primary endpoints. Thus, we deemed it necessary to consider that poor statistical correlation in evaluative

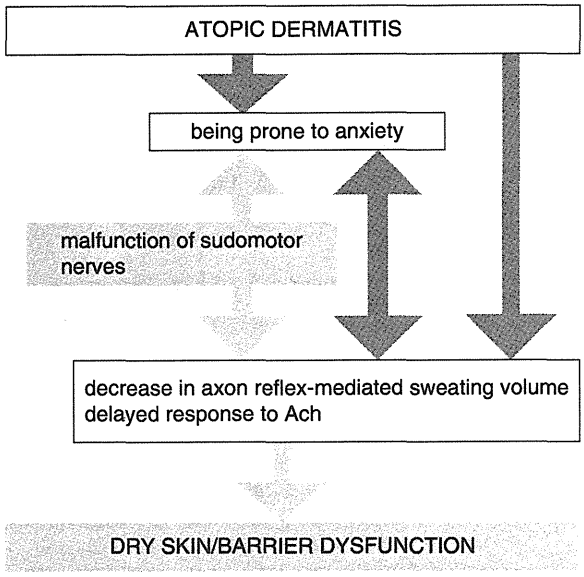

Fig. 4 Proposed association of abnormal sweating to dry skin and unique characteristics of AD. Dark gray arrows indicated the confirmatory results of this study. Light gray arrows indicated the tentative theory.

consequences did not mean no relation to each other.

In conclusion, this study revealed abnormal sweat responses in subjects with AD, and the higher the trait anxiety, the slower the sweat response. In contrast, previous report indicated rinsing old sweat on skin surface reduced severity of AD.[5] Put it all together, although there are arguments both for and against the involvement of "sweat" in the exacerbation of AD, our results suggest that studies of "sweat" should be divided into "sweating response" and "after sweating." From this point of view, we should give AD patients psychosomatic treatments and lifestyle guidance to stimulate adequate sweating. Additionally, we must endorse the importance of washing away sweat daily.[5]

ACKNOWLEDGEMENTS

This study is supported by the Ministry of Health, Labour and Welfare, Japan.

REFERENCES

1. Rieg S, Steffen H, Seeber S *et al.* Deficiency of dermcidin-derived antimicrobial peptides in sweat of patients with atopic dermatitis correlates with an impaired innate defense of human skin in vivo. *J Immunol* 2005;**174**:8003-10.
2. Schittek B, Paulmann M, Senyurek I, Steffen H. The role of antimicrobial peptides in human skin and in skin infectious diseases. *Infect Disord Drug Targets* 2008;**8**:135-43.
3. Eishi K, Lee JB, Bae SJ, Takenaka M, Katayama I. Impaired sweating function in adult atopic dermatitis: results of the quantitative sudomotor axon reflex test. *Br J Dermatol* 2002;**147**:683-8.
4. Schmid-Wendtner MH, Korting HC. The pH of the skin surface and its impact on the barrier function. *Skin Pharmacol Physiol* 2006;**19**:296-302.
5. Murota H, Takahashi A, Nishioka M *et al.* Showering reduces atopic dermatitis in elementary school students. *Eur J Dermatol* 2010;**20**:410-1.
6. Burry J, Coulson HF, Roberts G. Circadian rhythms in axillary skin surface pH. *Int J Cosmet Sci* 2001;**23**:207-10.
7. Hatano Y, Man MQ, Uchida Y *et al.* Maintenance of an acidic stratum corneum prevents emergence of murine atopic dermatitis. *J Invest Dermatol* 2009;**129**:1824-35.
8. Wessler I, Reinheimer T, Kilbinger H *et al.* Increased acetylcholine levels in skin biopsies of patients with atopic dermatitis. *Life Sci* 2003;**72**:2169-72.
9. Kindt F, Wiegand S, Niemeier V *et al.* Reduced expression of nicotinic alpha subunits 3, 7, 9 and 10 in lesional and nonlesional atopic dermatitis skin but enhanced expression of alpha subunits 3 and 5 in mast cells. *Br J Dermatol* 2008;**159**:847-57.
10. Lee JB, Bae JS, Matsumoto T, Yang HM, Min YK. Tropical Malaysians and temperate Koreans exhibit significant differences in sweating sensitivity in response to iontophoretically administered acetylcholine. *Int J Biometeorol* 2009;**53**:149-57.
11. Hanifin J, Rajka G. Diagnostic features of atopic eczema. *Acta Dermatol Venereol (Stockh)* 1980;**92**:44-7.
12. Saeki H, Furue M, Furukawa F *et al.* Guidelines for management of atopic dermatitis. *J Dermatol* 2009;**36**:563-77.
13. Severity scoring of atopic dermatitis: the SCORAD index. Consensus Report of the European Task Force on Atopic Dermatitis. *Dermatology* 1993;**186**:23-31.
14. Spielberger C, Gorsuch R, Lurshene R. *STAI-Manual for the State-Trait Anxiety Inventory ("Self-Evaluation Questionnaire")*. Palo Alto, CA, USA: Consulting Psychologists Press, 1970.
15. Sklan EH, Lowenthal A, Korner M *et al.* Acetylcholinesterase/paraoxonase genotype and expression predict anxiety scores in Health, Risk Factors, Exercise Training, and Genetics study. *Proc Natl Acad Sci U S A* 2004;**101**:5512-7.
16. Hashizume H, Horibe T, Ohshima A, Ito T, Yagi H, Takigawa M. Anxiety accelerates T-helper 2-tilted immune responses in patients with atopic dermatitis. *Br J Dermatol* 2005;**152**:1161-4.
17. Oh SH, Bae BG, Park CO *et al.* Association of stress with symptoms of atopic dermatitis. *Acta Derm Venereol* 2010; **90**:582-8.
18. Hashmonai M, Kopelman D, Assalia A. The treatment of primary palmar hyperhidrosis: a review. *Surg Today* 2000; **30**:211-8.

Intrauterine sensitization of allergen-specific IgE analyzed by a highly sensitive new allergen microarray

Norio Kamemura, MSc,[a] Hitomi Tada, MSc,[a] Naoki Shimojo, MD, PhD,[b] Yoshinori Morita, MD, PhD,[b] Yoichi Kohno, MD, PhD,[b] Takao Ichioka, MD,[c] Koichi Suzuki, MSc,[a] Kenji Kubota, MSc,[a] Mineyoshi Hiyoshi, PhD,[a] and Hiroshi Kido, MD, PhD[a] *Tokushima, Chiba, and Naruto, Japan*

Background: To design a rational allergy prevention program, it is important to determine whether allergic sensitization starts *in utero* under the maternal immune system.
Objective: To investigate the origin of allergen-specific IgE antibodies in cord blood (CB) and maternofetal transfer of immunoglobulins.
Methods: The levels of food and inhalant allergen-specific IgE, IgA, IgG, and IgG_4 antibodies in CB and maternal blood (MB) from 92 paired neonates and mothers were measured by using a novel allergen microarray of diamond-like-carbon–coated chip, with high-sensitivity detection of allergen-specific antibodies and allergen profiles.
Results: The levels of allergen-specific IgE antibodies against food and inhalant allergens and allergen profiles were identical in CB and newborn blood, but the levels and profiles, specifically against inhalant allergens, were different from those in MB. The level of allergen-specific IgA antibodies was below the detection levels in CB despite clear detection in MB. Therefore, contamination with MB in CB was excluded on the basis of extremely low levels of IgA antibodies in CB and the obvious mismatch of the allergen-specific IgE and IgA profiles between CB and MB. However, the levels of allergen-specific IgG and IgG_4 antibodies and their allergen profiles were almost identical in both MB and CB.
Conclusion: Allergen-specific levels of IgE and IgA antibodies and their allergen profiles analyzed by the diamond-like-carbon allergen chip indicate that IgE antibodies in CB are of fetal origin. Food-allergen specific IgE antibodies were detected more often than inhalant-allergen specific IgE antibodies in CB, the reason of which remains unclarified. (J Allergy Clin Immunol 2012;130:113-21.)

Key words: Prenatal, allergen-specific IgE, IgA, IgG, and IgG_4, sensitization, cord blood, allergen chip

Newborns sometimes show measurable amounts of IgE antibodies in cord blood (CB), and a relatively high level of total IgE is often regarded a prenatal risk factor for atopic propensity in the newborn.[1-5] The latter conclusion is supported by the detection of allergen-specific IgE[6,7] and allergen-specific T-cell memory[8-10] in CB and suggests that primary sensitization can occur transplacentally *in utero*. However, the timing of allergen sensitization is still controversial, with conflicting evidence suggesting transplacental priming[6] versus postnatal priming.[11,12]

These conflicting conclusions could be due to the following background including the methods of analysis: (1) High probability of maternal blood (MB) contamination during CB sampling or through small placental bleeding during late pregnancy or delivery. (2) Low-sensitivity detection of allergen-specific IgE levels and allergen-specific IgE profiles against various food and inhalant allergens in CB. Since the majority of total IgE in CB is nonspecific IgE, generally much higher than allergen-specific IgE levels,[11,13,14] the detection of allergen-specific IgE and its profiles of CB are difficult, highlighting the need for the development of new highly sensitive methods for the detection of allergen-specific antibodies. In a recent study,[15] we described a new microarray technique of high-density antigen immobilization using the carboxylated arms on the surface of a diamond-like-carbon (DLC)-coated chip, which had higher sensitivity in detecting allergen-specific IgE, IgA, IgG, and IgG_4 compared with the UniCAP system and allergen-specific immunoglobulin profiles against various food and inhalant allergens.

The present study is an extension to our previous study[15] and was designed to further examine the utility of the new method. Specifically, we used the DLC chip to detect allergen-specific IgE, IgA, IgG, and IgG_4 and determine the allergen profiling patterns in carefully sampled CB to avoid MB contamination. The new technique identified allergen-specific IgE antibodies in CB, which were of fetal origin. The results allowed analysis of the mechanism of allergen sensitization in the fetus and maternofetal transfer of immunoglobulins.

METHODS

Subjects

The study included 92 healthy paired pregnant women and their newborns recruited at Kawatetu-Chiba Hospital, Chiba University Hospital, and Health Insurance Naruto Hospital from January 2007 to May 2008 in Japan. At birth, CB was collected by needle puncture of the umbilical vein after careful

From [a]the Division of Enzyme Chemistry, Institute for Enzyme Research, University of Tokushima, Tokushima; [b]the Department of Pediatrics, Graduate School of Medicine, Chiba University, Chiba; and [c]the Health Insurance Naruto Hospital, Naruto.

Supported in part by Grants-in-Aid 18659293, 21659245, and 19659253 from the Ministry of Education, Culture, Sports, Science, and Technology; by Health and Labor Sciences Research Grants of the Research on Allergic Diseases and Immunology (grant no. 21200501) from the Ministry of Health, Labor and Welfare; and by the supporting program for creating university ventures from Japan Science and Technology Agency of Japan.

Disclosure of potential conflict of interest: The authors declare that they have no relevant conflicts of interest.

Received for publication November 8, 2011; revised January 24, 2012; accepted for publication February 15, 2012.

Available online March 30, 2012.

Corresponding author: Hiroshi Kido, MD, PhD, Division of Enzyme Chemistry, Institute for Enzyme Research, University of Tokushima, Kuramoto-cho 3-18-15, Tokushima 770-8503, Japan. E-mail: kido@ier.tokushima-u.ac.jp.

0091-6749/$36.00

doi:10.1016/j.jaci.2012.02.023

Abbreviations used
BU: Binding unit
CB: Cord blood
DLC: Diamond-like-carbon
MB: Maternal blood
NB: Neonatal blood

cleaning of the umbilical cord to avoid MB contamination. Neonatal blood (NB) was obtained at the time of birth by Contact-Activated Lancets low flow (BD Microtainer, Franklin Lakes, NJ), and venous MB was obtained at 4 to 5 days after delivery. Blood samples were then centrifuged at 150 × *g* for 10 minutes to prepare serum. Serum was frozen at −30°C until analysis. All subjects provided written informed consent to participate in this study. This study was approved by the ethics committees of the Graduate School of Medicine, Chiba University, and Tokushima University Hospital.

Allergen chip assay

Allergen-specific IgE, IgA, IgG, and IgG_4 levels were measured in serum by the allergen diagnosis DLC chip as described in detail previously.[15] Briefly, carboxylated DLC film-coated glass slide (Gene slide) was purchased from Toyo Kohan Co (Tokyo, Japan). Natural allergens *Dermatophagoides farinae* and *Dermatophagoides pteronyssinus* were purchased from Allergon (Ängelholm, Sweden). Purified single allergens as molecular allergens, such as ovomucoid, ovalbumin, conalbumin, α-casein, β-casein, and β-lactoalbumin, were purchased from Sigma-Aldrich (St Louis, Mo). Japanese cedar was purchased from Cosmo Bio Co (Tokyo, Japan) and house dust from GREER (Lenoir, NC). Human serum IgE (75/502), IgG, IgA, and IgM (67/086) used as internal standards on chip were from the National Institute for Biological Standards and Control (Hertfordshire, United Kingdom).

After the activation of carboxylated DLC slides and the fabrication of allergen microarray, the individual arrays were incubated with 20 μL of 1:2 to 1:50 diluted serum as the primary antibody, then reacted with a HiLyte Fluor 555 (Dojindo Molecular Technologies, Inc, Kumamoto, Japan)-labeled secondary antibody against each human IgE, IgA, IgG, and IgG_4, and the resulting images were analyzed as described previously.[15] On each allergen chip, various concentrations of human IgE, IgG, or IgA were spotted as internal standards. From the cubic equation of IgE, IgG, or IgA standard concentrations, the amounts of allergen-specific antibodies bound to allergen on the chips were calculated and expressed as binding unit (BU). The BUs of IgE, IgA, IgG, and IgG_4 were reported as BUe, BUa, BUg, and BUg4, respectively. The detection limit of allergen-specific IgE against various natural and molecular allergens in serum in the DLC chip was 10 BUe/mL, which corresponds to about 0.07 IU/mL of the UniCAP system, indicating about 4 to 8 times higher sensitivity for the DLC chip than for the UniCAP system. The UniCAP system has a limit of 0.35 IU/mL for IgE detection.[6,16] The detection limits for allergen-specific IgA, IgG, and IgG_4 were 0.25 BUa, 2.50 BUg, and 0.53 BUg4, respectively.

We compared the sensitivity of the DLC chip with that of the UniCAP system for allergen-specific IgE in CB, which contains a relatively high level of nonspecific IgE antibodies[11,13,14] (Table I). The UniCAP system did not detect allergen-specific IgE antibodies in all CB samples analyzed in our experiments, even in samples of fluorescence units (BUe/mL) of more than 18 to 22 times the detection limit (10 BUe/mL) on the DLC chip. However, the difference in the sensitivity between the DLC chip and the UniCAP system using MB samples was equivalent to that in allergic patients[15] described above.

Total IgA assay

Total IgA concentration was determined by using an ELISA kit (Bethyl Laboratories, Montgomery, Tex) according to the protocol provided by the manufacturer. The chromogen produced was measured at an absorbance of 450 nm by using a SpectraMax Plus384 autoreader (Molecular Devices Corp, Sunnyvale, Calif).

TABLE I. Comparison of assay sensitivity in detecting antigen-specific IgE in CB and MB against food allergens and inhalant allergens using the DLC chip system and the UniCAP system

	CB (1:1 dilution)		MB (1:1 dilution)	
Allergen	DLC chip (BUe/mL)	UniCAP (Ua/mL)	DLC chip (BUe/mL)	UniCAP (Ua/mL)
Food				
Egg white	30.35	ND*	77.41	0.545
	11.02	ND	23.65	ND
Ovomucoid	180.0	ND	134.8	0.960
	84.89	ND	64.66	ND
	13.30	ND	23.15	ND
Milk	221.4	ND	182.7	1.095
	30.90	ND	61.71	0.540
	18.05	ND	23.15	ND
Inhalant				
Cedar pollen	55.55	ND	90.98	0.960
	21.78	ND	32.20	ND
Df	54.01	ND	80.76	1.275
	47.38	ND	25.53	ND
Dp	63.04	ND	215.6	2.950
	26.48	ND	60.70	ND

CB serum (1:1 dilution) and MB serum (1:1 dilution) were used for the measurement of allergen-specific IgE levels on the UniCAP system and the DLC chip. Detection limit on the DLC chip: 10 BUe/mL.
Df, Dermatophagoides farinae; Dp, Dermatophagoides pteronyssinus; Ua, arbitrary unit.
**ND,* Not detectable of UniCAP assay: <.35.

Statistical analysis

Statistical analysis was conducted by using the Statistical Package for Social Sciences (version18.0; SPSS, Inc, Chicago, Ill). Most data sets showed skewed distribution, and thus Spearman's rank correlation test was used to assess the relationship between the different samples. A P value of ≤.05 was considered significant.

RESULTS

Allergen-specific serum IgE, IgA, IgG, and IgG_4 levels and their profiles in CB, NB, and MB

Allergen-specific IgE, IgA, IgG, and IgG_4 levels in CB, NB, and MB and their profiles were analyzed by using the allergen diagnosis DLC chips. The DLC chip detected more than 1 allergen-specific IgE of the tested 11 allergens in 83.7% of CB (n = 92). Fig 1 shows allergen-specific IgE, IgA, IgG, and IgG_4 profiles in representative paired CB, NB, and MB samples. MB contained high-reactive IgE levels against inhalant allergens *Dermatophagoides pteronyssinus* and *Dermatophagoides farinae* and moderate-reactive IgE levels against food allergens milk, α-casein, and β-casein and also inhalant allergens cedar pollen and house dust. CB, however, did not contain any reactive IgE levels against inhalant allergens *Dermatophagoides pteronyssinus*, *Dermatophagoides farinae*, cedar pollen, and house dust, but it had moderate-reactive IgE levels against food allergens milk, α-casein, β-casein, and ovomucoid. Although MB contained various allergen-specific IgA antibodies, CB did not show any reactive IgA. Almost identical levels of allergen-specific IgG and IgG_4 antibodies to each allergen and similar profile patterns were observed among MB, NB, and CB. The difference in the allergen-specific profiles of IgA and IgE between MB and CB or NB indicates no MB contamination in the paired CB samples and suggests that allergen-specific IgE antibodies in CB are derived from the fetus. The almost identical allergen-reactive

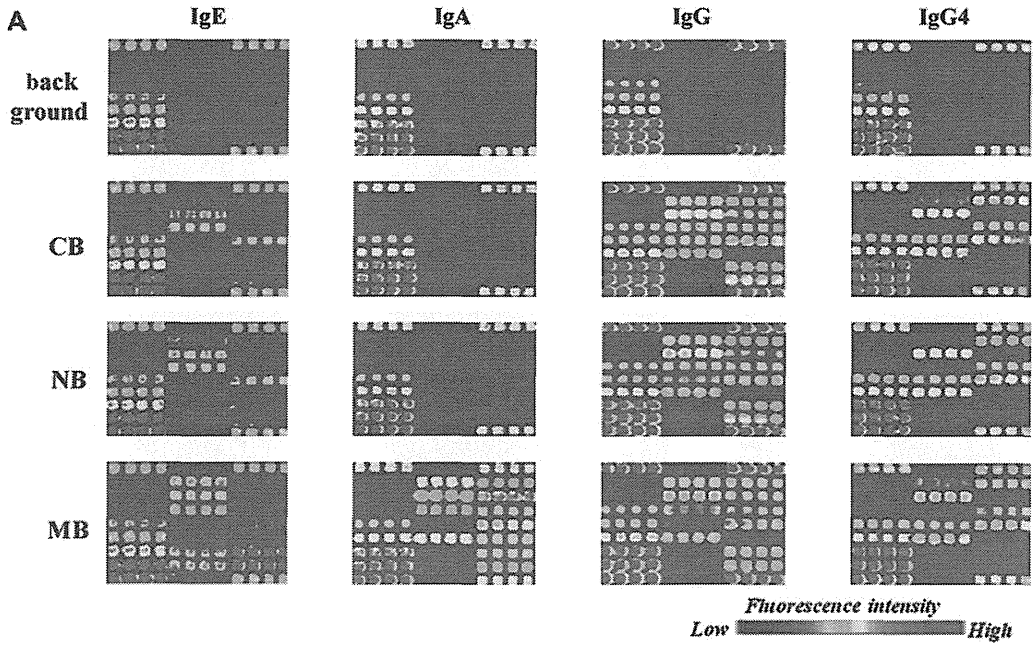

B

GD	Blank	GD
Blank	Milk	Egg white
Std	α-Casein	Egg yolk
	β-Casein	Ovalbumin
	α-Lactoalbumin	Ovomucoid
	β-Lactoglobulin	Conalbumin
	Cedar pollen	Dp
	House dust	Df
	Blank	GD

FIG 1. Multiallergen-specific profiling patterns of IgE, IgA, IgG, and IgG_4 in paired CB, NB, and MB analyzed by the DLC chip. **A,** Rainbow displays of fluorescence intensities of allergen-specific IgE, IgA, IgG, and IgG_4 reactivities against allergens of an array probed sera of paired CB, NB, and MB. **B,** Layout of the allergen DLC chip. *Df, Dermatophagoides farinae; Dp, Dermatophagoides pteronyssinus; GD,* guideline dot by standard serum; *Std,* standard calibration of human serum IgE from the National Institute for Biological Standards and Control. Each allergen was spotted in quadruple on the chip. Results are representative of 1 pair of 92 samples.

profiles of IgG and IgG_4 among CB, NB, and MB support the established finding of maternofetal transfer of IgG.[17] Similar findings were observed in the other 91 paired CB and MB samples.

To evaluate the cross-reactivity of the antigen-IgE antibody reaction on the highly sensitive DLC chip, serum was preincubated with each allergen for 2 hours at 37°C followed by allergen-specific IgE detection on the chip (Fig 2). Each allergen selectively and almost completely adsorbed allergen-specific IgE antibodies without any interference or cross-reactivity by other antigen-antibody reactions. These results indicate that allergen-specific IgE was selectively detected on the DLC chip.

Total IgA levels in CB and MB

Since the total IgA level in CB is generally used as an indicator of transfer of MB,[18] we measured total IgA levels in CB and MB by using ELISA. Total IgA levels in all CB were within the minimal levels between 1.2 and 19.4 μg/mL (Fig 3) and no allergen-specific IgA was detected (Fig 1 and Table II). In contrast, total IgA levels in MB were between 0.8 and 3.5 mg/mL. Therefore, the total IgA levels in MB did not correlate with those in CB. These results indicate that MB contamination is below the detection level in CB collected by careful needle puncture of the umbilical vein.

Allergen-specific IgE, IgA, IgG, and IgG_4 levels in CB and MB

Allergen-specific IgE, IgA, IgG, and IgG_4 levels were analyzed in 92 paired CB and MB samples. The proportion of CB samples positive for allergen-specific IgE against each food allergen (using a cutoff value of 10 BUe) ranged from 6.5% to 69.6%, with the highest proportion for ovomucoid, while the proportion of samples positive for each inhalant allergen ranged between 6.5% and 28.3% (Table II). The proportions of MB samples positive for allergen-specific IgE against each food allergen were almost similar to those of CB. In contrast, the proportions of MB samples positive for allergen-specific IgE against inhalant allergens were considerably higher (between 72.8% and 84.8%) than those of CB. Specifically, the proportion of CB samples positive for allergen-specific IgE

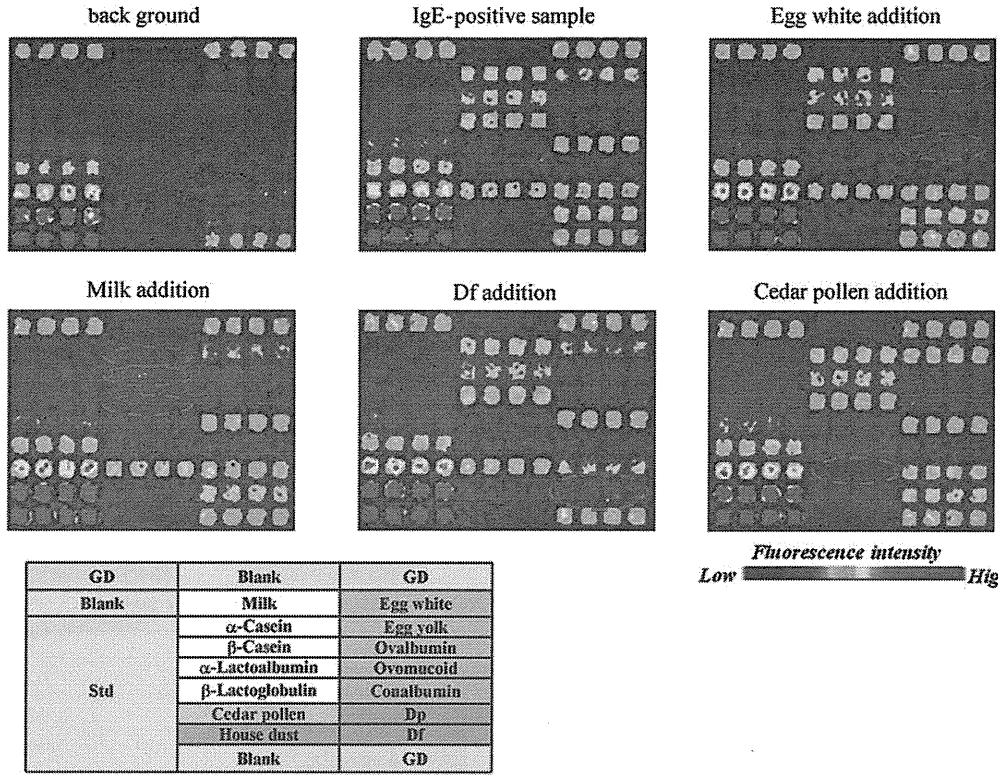

FIG 2. Allergen-specific IgE adsorption for evaluating cross-reactivity of antigen-IgE antibody reaction on the DLC chip. MB sample containing allergen-specific IgE against both food and inhalant allergens was preincubated with egg white (5 μg/mL), milk (5 μg/mL), Df (500 μg/mL), or cedar pollen (500 μg/mL) at 37°C for 2 hours. After the reaction, each sample was centrifuged at 17,500 × *g* for 30 minutes to remove antigen-antibody complex, and then the supernatant was used for multiallergen profiling of IgE on the DLC chip. Bottom, layout of the allergen on the DLC chip. *Df, Dermatophagoides farinae; Dp, Dermatophagoides pteronyssinus; GD,* guideline dot; *Std,* standard calibration of human serum IgE.

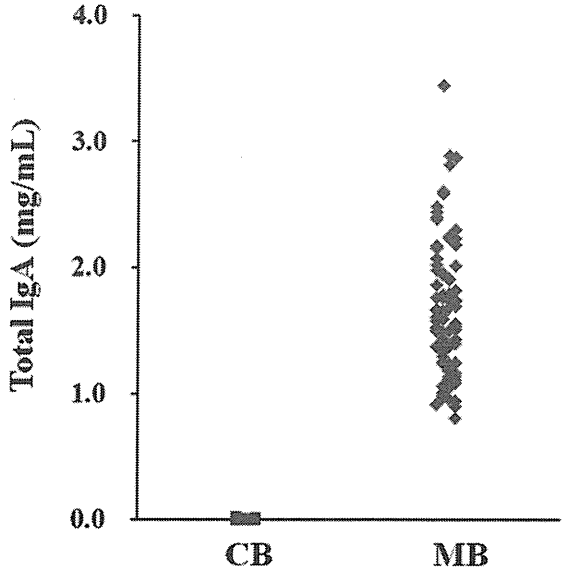

FIG 3. Total IgA levels in CB and MB. Total IgA levels in CB and MB (n = 92) were analyzed by ELISA.

with IgE-positive MB only against each food allergen was high and the mean value was 86.4%. The mean BU ratio for CB/MB in IgE-positive subjects only against the food allergens (ie, CB BUe/MB BUe; Table II) was 1.24 ± 0.60. In contrast, the proportion of CB samples positive for allergen-specific IgE in the IgE-positive MB subjects only against the inhalant allergens was lower (range, 9.0%-33.8%), with a mean value of 20.7%. The mean BU ratio for CB/MB in the IgE-positive subjects only against inhalant allergens (ie, CB BUe/MB BUe; Table II) was 0.54 ± 0.50. These results suggest a potentially greater sensitization against food allergens than against inhalant allergens *in utero*.

The levels of allergen-specific IgA against the allergens tested in CB were below the detection limits, but the proportion of MB samples positive for allergen-specific IgA against food and inhalant allergens ranged between 7.6% and 77.2%, with the highest value against milk (Table II). A fairly similar or identical trend was noted in CB and MB for allergen-specific IgG against food and inhalant allergens (Table III). The mean proportions of CB samples positive for allergen-specific IgG against food and inhalant allergens in subjects with IgG-positive MB only were 91.2% and 87.3%, respectively, and the mean BU ratios of CB/BM in the IgG-positive subjects only (CB BUg/MB BUg; Table III) against food and inhalant allergens were 1.08 ± 0.38 and 0.87 ± 0.24, respectively. The similar proportions of CB and MB samples and BU ratios around 1.0 indicate maternofetal transfer of allergen-specific IgG.

Although the mean proportion of allergen-specific IgG_4-positive CB in the IgG_4-positive MB subjects only against food

TABLE II. Allergen-specific IgE and IgA values in paired CB and MB samples, and BU ratio and correlation between CB- and MB-positive only

	CB (n = 92)		MB (n = 92)		CB/MB-positive only				
IgE positive in:	**n**	**Percent***	**n**	**Percent***	**n**	**Percent†**	**BU ratio‡ (CB BUe/MB BUe ± SD)**	**Correlation between CB and MB (r_s)§**	***P* value**
Food									
α-Casein	28	30.4	25	27.2	18	72.0	1.09 ± 0.60	0.63	.005
β-Casein	16	17.4	15	16.3	11	73.3	1.10 ± 0.63	0.69	.002
α-Lactoalbumin	6	6.5	1	1.1	1	100	0.95 ± 0.00	NA	
β-Lactoglobulin	15	16.3	5	5.4	5	100	1.26 ± 0.65	0.30	.006
Ovalbumin	34	37.0	12	13.0	11	91.7	1.44 ± 0.70	0.44	.180
Ovomucoid	64	69.6	55	59.8	55	100	1.89 ± 0.82	0.89	<.001
Milk	18	19.6	22	23.9	12	54.5	1.14 ± 0.54	0.87	<.001
Egg white	23	25.0	8	8.7	8	100	1.06 ± 0.25	0.81	<.001
Mean						86.4	1.24 ± 0.60		
Inhalant									
Cedar pollen	6	6.5	67	72.8	6	9.0	0.34 ± 0.16	0.83	.042
Df	26	28.3	74	80.4	25	33.8	0.59 ± 0.58	0.06	.830
Dp	18	19.6	78	84.8	15	19.2	0.70 ± 0.74	0.21	.300
Mean						20.7	0.54 ± 0.50		

	CB (n = 92)		MB (n = 92)		CB/MB-positive only				
IgA positive in:	**n**	**Percent***	**n**	**Percent***	**n**	**Percent†**	**BU ratio‡ (CB BUa/MB BUa ± SD)**	**Correlation between CB and MB (r_s)§**	***P* value**
Food									
α-Casein	0	NA	46	50.0	0	NA	NA	NA	
β-Casein	0	NA	50	54.3	0	NA	NA	NA	
α-Lactoalbumin	0	NA	7	7.6	0	NA	NA	NA	
β-Lactoglobulin	0	NA	15	16.3	0	NA	NA	NA	
Ovalbumin	0	NA	17	18.5	0	NA	NA	NA	
Ovomucoid	0	NA	19	20.7	0	NA	NA	NA	
Milk	0	NA	71	77.2	0	NA	NA	NA	
Egg white	0	NA	16	17.4	0	NA	NA	NA	
Mean									
Inhalant									
Cedar pollen	0	NA	21	22.8	0	NA	NA	NA	
Df	0	NA	35	38.0	0	NA	NA	NA	
Dp	0	NA	26	28.3	0	NA	NA	NA	
Mean									

Df, Dermatophagoides farinae; *Dp, Dermatophagoides pteronyssinus*; *NA,* not available due to lack of positive cases.
*Percentages of allergen-specific IgE- and IgA-positive samples.
†Percentages of allergen-specific IgE- and IgA-positive samples from MB-positive only.
‡BU ratios (CB BUe/MB BUe, CB BUa/MB BUa).
§Correlation coefficient analyzed Spearman's rank correlation test (r_s, *P* value) of allergen-specific IgE and IgA-positive CB and MB-positive only.

allergens was 96.0%, those against inhalant allergens was below the detection levels in the samples tested (Table III). The mean BU ratio between IgG_4-positive CB and IgG_4-positive MB subjects only (CB BUg4/MB BUg4) against food allergens was 0.99 ± 0.39. The results add support to the notion of maternofetal transfer of allergen-specific IgG_4.

Correlation of allergen-specific IgE, IgA, IgG, and IgG_4 between CB and MB

The results of correlation analysis of allergen-specific IgE, IgA, IgG, and IgG_4 levels (BU) between paired CB and MB samples (n = 92) determined by the DLC chip are shown in Table IV. There were strong correlations for allergen-specific IgE levels against food allergens between CB and MB with considerably high correlation coefficients (range, 0.53-0.94; $P < .001$), with the exception of weak correlation for α-lactoalbumin at 0.37 ($P < .001$). In contrast, the correlation coefficients for inhalant allergens were low (range, 0.01-0.30). In addition, there were strong correlations for allergen-specific IgE against crude allergens between CB and MB in the IgE-positive MB subjects only (Table II), such as milk, egg white, and cedar pollen, with high correlation coefficients of 0.87 ($P < .001$), 0.81 ($P < .001$), and 0.83 ($P < .042$), respectively. The correlation profiles of allergen-specific IgE against various food and inhalant allergens for CB and MB are depicted in Fig 4.

There were also significant and strong correlations for allergen-specific IgG against food and inhalant allergens between CB and MB ($r_s > 0.74$; $P < .001$), except allergen-specific IgG against cedar pollen and α-lactoalbumin (r_s, not available) and against β-lactoglobulin ($r_s = 0.58$; $P < .001$) (Table IV). There were also strong correlations for allergen-specific IgG_4 against food allergens between CB and MB ($r_s > 0.85$; $P < .001$), although that for allergen-specific IgG_4 against α-lactoalbumin was weaker ($r_s = 0.68$; $P < .001$). The correlation